Weather and climate extremes in a changing Arctic

Xiangdong Zhang[1,2,†], Timo Vihma[3], Annette Rinke[4], G.W.K. Moore[5], Han Tang[2], Cecilia Äijälä[6], Alice DuVivier[7], Jianbin Huang[8,9], Laura Landrum[7], Chao, Li[10,11], Jing Zhang[12], Linette Boisvert[13], Bin Cheng[3], Judah Cohen[14,15], Dörthe Handorf[4], Edward Hanna[16], Katharina Hartmuth[17], Marius O. Jonassen[18], Yong Luo[19], Sonja Murto[20,21,22], James E. Overland[23], Chelsea Parker[13,24], William Perrie[25], Kirstin Schulz[26], Axel Schweiger[27], Thomas Spengler[28,29], Michael Steele[26], Wen-wen Tung[30], Nicholas Tyrrell[3,31], Elina Valkonen[13,24], Hailong Wang[32], Zhuo Wang[33], Wilbert Weijer[34,35], Siiri Wickström[36], Yutian Wu[37], and Minghong Zhang[38]

[1]North Carolina Institute for Climate Studies, North Carolina State University, Asheville, NC, USA.
[2]Department of Marine, Earth and Atmospheric Sciences, North Carolina State University, Raleigh, NC, USA.
[3]Finnish Meteorological Institute, Helsinki, Finland.
[4]Alfred Wegener Institute, Helmholtz Centre for Polar and Marine Research, Potsdam, Germany.
[5]Department of Physics, University of Toronto, Toronto, ON, Canada.
[6]INAR/Physics, University of Helsinki, Helsinki, Finland.
[7]NSF-National Center for Atmospheric Research, Boulder, CO, USA.
[8]Beijing Yanshan Earth Critical Zone National Research Station, University of Chinese Academy of Sciences, Beijing, China.
[9]College of Resources and Environment, University of Chinese Academy of Sciences, Beijing, China.
[10]Key Laboratory of Geographic Information Science, Ministry of Education, East China Normal University, Shanghai, China.
[11]School of Geographic Sciences, East China Normal University, Shanghai, China.
[12]Department of Physics, North Carolina A&T State University, Greensboro, NC, USA.
[13]Cryospheric Sciences Lab, NASA Goddard Space Flight Center, Greenbelt, MD, USA.
[14]Atmospheric and Environmental Research, Lexington, MA, USA.
[15]Department of Civil and Environmental Engineering, Massachusetts Institute of Technology, Cambridge, MA, USA.
[16]Department of Geography, University of Lincoln, Lincoln, UK.
[17]Institute for Atmospheric and Climate Science, ETH Zurich, Zurich, Switzerland.
[18]Arctic Geophysics Department, The University Centre in Svalbard, Longyearbyen, Norway.
[19]Department of Earth System Science, Tsinghua University, Beijing, China.
[20]Department of Meteorology, Stockholm University, Stockholm, Sweden.
[21]Bolin Centre for Climate Research, Stockholm University, Stockholm, Sweden.
[22]Department of Earth Sciences, Uppsala University, Uppsala, Sweden.
[23]National Oceanic and Atmospheric Administration/Pacific Marine Environmental Laboratory, Seattle WA, USA.
[24]Earth System Science Interdisciplinary Center, University of Maryland, College Park, MD, USA.
[25]Fisheries and Oceans Canada, Bedford Institute of Oceanography, Dartmouth, NS, Canada.
[26]Oden Institute for Computational Engineering and Sciences, The University of Texas at Austin, Austin, TX, USA.
[27]Applied Physics Lab, Polar Science Center, University of Washington, Seattle, WA, USA.
[28]Geophysical Institute, University of Bergen, Bergen, Norway.
[29]Bjerknes Centre for Climate Research, Bergen, Norway.
[30]Department of Earth, Atmospheric, and Planetary Sciences, Purdue University, West Lafayette, IN, USA.
[31]Bureau of Meteorology, Melbourne, VIC, Australia
[32]Pacific Northwest National Laboratory, Richland, WA, USA.
[33]Department of Climate, Meteorology, & Atmospheric Sciences, University of Illinois at Urbana-Champaign, Urbana, IL, USA.
[34]Los Alamos National Laboratory, Los Alamos, NM, USA.

[35]International Arctic Research Center, University of Alaska Fairbanks, Fairbanks, AK, USA.
[36]Department of Arctic Technology, The University Centre in Svalbard, Longyearbyen, Norway.
[37]Lamont-Doherty Earth Observatory, Columbia University, Palisades, NY, USA.
[38]Department of Physics and Atmospheric Sciences, Dalhousie University, Halifax, NS, Canada.

[†]**e-mail:** xzhan238@ncsu.edu

Abstract
Weather and climate extremes are increasingly occurring in the Arctic. In this Review, we evaluate historical and projected changes in rare Arctic extremes across the atmosphere, cryosphere and ocean, and elucidate their driving mechanisms. Comparison of probability density functions pre- and post-2000 highlights clear shifts in the mean and extreme distributions. Indeed, the frequency and amplitude of extremes consistently increased since the turn of the 21st century, with probability increase by 20.0% for atmospehric heatwaves; 76.7% for Atlantic layer warm events; 83.5% for sea ice extent loss; and 62.9% for Greenland Ice Sheet melt extent. These changes can be explained using a 'pushing and triggering' concept, representing interplay between external forcing and internal variability: long-term warming destabilizes the climate system and 'pushes' it to a new state, allowing subsequent variability associated with large-scale atmosphere-ocean-ice interactions and synoptic systems to 'trigger' extreme events over different timescales. The apparent increase in extremes ~2000. Ongoing anthropogenic warming is expected to further increase the frequency and magnitude of extremes, such that probability increases by 72.6% for atmospehric heatwaves; 68,7% for Atlantic layer warm events; and 93.3% for Greenland Ice Sheet melt rate at the end of this century. A summer ice-free would occur in the mid century. Future research should prioritize the development of physically-based metrics, enhance high-resolution observation and modeling capabilities, and improve understanding of multiscale Arctic climate drivers.

[H1] Introduction

The Arctic climate is rapidly changing along with the increasing greenhouse gases forcing. These changes are typified by Arctic amplification, describing an annual mean Arctic warming rate that is more than 3x that of the global average from 1979-2023 (0.68 ºC dec^{-1} vs. 0.20 ºC dec^{-1}; north of 60ºN)[1–5]. In conjunction with the amplified long-term, quasi-linear warming trend, Arctic climate changes also exhibit a highly non-linear trajectory due to its nonlinear interactions with the occurrence of weather and climate extremes. Extreme events, including record-breaking extemes, have consistently occurred across all components of the Arctic climate system with an increased frequency since the turn of the 21st century, sheding light on a shift of the Arctic climate system into a new state. These events include: atmospheric and marine heat waves[6–10], rapid sea ice loss[6,11–13], heavy precipitation[14–16], rain-on-snow events[17–20], strong winds[21–24], pulses of the Atlantic and Pacific warm water anomalies[6,25–28], and Greenland Ice Sheet (GrIS) melt[29–31], amongst others (**Fig. 1**). In 2012, for instance, the surface air temperature anomalies exceeded 10.0℃ in February over much of the Arctic, the GrIS melt at or near the surface unprecendently occurred across 98.6 % of the ice sheet in summer, and sea ice retreated to about 50.0 % of it's climatological position in September.

These extremes have substantial impacts across the coupled Earth system. For example, winter heatwave and summer sea ice loss events, like those occurring in 2012, can considerably change the habitat of marine life, influencing the distribution of species, biodiversity, and food web. The significant loss of sea ice exposes coastline to storm surge, causing coastal flooding, exacerbating coastal erosion, and finally endangering coastal communities and infrustructures. The extreme GrIS melt in summer 2012 also resulted in an intense runoff, destroying bridges and other infrustructures across and adjacent to the Watson River near Kangerlugssuaq. Moreover, such extreme events could strengthen climate feedback processes between the atmosphere, ocean and cryosphere, specifically albedo feedback, water vapor feedback, and cloud feedback. These feedback processes could, in turn, accelerate Arctic climate change and reduce resilience of the Arctic

climate system due to their roles in enhancing greenhouse gases forced changes. Yet, the effects of Arctic extremes (and corresponding contributions to longer-term changes) are not locally constrained—what happens in the Arctic doesn't stay in the Arctic. They contribute to global-mean warming[1], and remotely force midlatitude weather and climate extremes via Arctic amplification forced changes in the atmospheric circulation dynamics, such as a phase transition or a spatial shift of the dominant circulation pattern, amplified jet streams, and weakened stratospheric polar vortex[1,32–34].

Despite their local and global importance, understanding of Arctic extremes and their dramatic increase in the frequency and intensity since the beginning of the century is less established. Knowledge in the Arctic is strongly influenced by paucity of data, due to its harsh environment and limited accessibility. The short records of observations with sparse coverage, therefore, prevent from realistically capturing complete temporal and spatial strucutres of climate system state and extreme events. All of these also raises a grand challenge for accurately describing and representing the associated physical processes, especially at high resolutions, in Earth system models. Moreover, unique and complicated dynamics and thermodynamics, as well as their incomplete representation in Earth system models, have translated into inconsistencies and discrepancies in understanding and simulating their underlying physical mechanisms[12,13,35–37]. Yet, knowledge of the observed and projected changes in Arctic extremes, as well as their driving mechanimss, are vital to enhancing the capabilities for predicting Arctic weather and climate extrems and facilitating mitigation and adaptation planning and decision-making for building a climate-ready society and economy.

In this Review, we synthesize the state-of-knowledge of Arctic weather and climate extremes. We begin by summarizing observed Arctic extremes that have systematically and consistently occurred across the atmosphere, ocean and cryosphere. Next, we discuss how multiscale drivers and associated interactive processes work together to produce systematic increases in the frequency and intensity of Arctic extremes. Consideration then turns to future projections of extremes under anthropogenic warming, before identifying and making recommendations to advance the field. Throughout, focus is placed on rare extreme events[38]—those that exceed the range of normal interannual variability or historical records, in this case by 1.5 or 1.0 standard deviations depending on the nature of the climate components. These rare extreme events are selected over the more typical local- and timescale-specific extremes. (for example, daily and monthly temperautre and preciptiaion extremes owing to their exceedance over the criterion and higher frequency of variability; monthly, seasonal or annual ocean and cryosphere extremes considering their longer memory and limited high temporal resolution data avaiablility). These rare events coherently occur across and then enhance interactions between the components of the Arctic climate system, amplifying systematic changes and having high environmental and socio-econimic impacts. Consideration is also only given to ocean-, sea ice- and ice sheet -dominated areas, excluding complex terrestrial regions which are closely connected to and governed by midlatitude dynamics and processes.

[H1] Observed Arctic weather and climate extremes

Weather and climate extremes have been been observed across all components of the Arctic climate system, with increasing frequency and intensity since the beginning of the 21st century[6–9,11–15,39]. Here, observed Arctic atmosphere (heat, precipitation and wind), ocean (heat transport and temperautre at different key depths) and cryosphere (sea ice retreat and GrIS melt) extremes are examined. Discussion is focused on specific rare events, changes in their probability pre-2000 and post-2000, and their trends (**Fig. 2**).

[H2] Atmosphere

[H3] Temperature

Substantial changes have been observed in Arctic winter surface air temperature (SAT). Indeed, the probability density function (PDF) distributions comparing 1979/80-1999/2000 and 2000/01-2023/24 indicate a clear shift toward warmer daily SAT in the North Atlantic Arctic (**Fig. 2a**, **left**), where the highest frequency of rare extreme winter heatwave events have occurred. This shift includes both the mean climate state and the extreme end of the distributions, suggesting an increase in the maximum probability of rare

daily extreme events from 8.2% to 28.2% using the +1.5 standard devation for 1979/80-1999/2000 as the threshold (**Table 1**). A striking, landmark rare extreme heatwave occurred in winter 2005/06[6]. Since then, rare extreme winter heatwaves have consecutively occurred with an increased frequency and intensity[7–9,39]. During one of these events occurring in 2015/16, SAT at the north pole increased 26°C (from -26.8°C to -0.8°C) from the 29-30 December as revealed by drifting buoy observations[7,40]. In the same event, two-dimensional reanalysis datasets also shows a large magnitude of SAT increase on 1- 2 January 2016, reaching anomalies of 7-8°C >65°N[9,41,42]. Although rare daily warm extremes are most prominent in the Atlantic Arctic (in many cases reaching melting point), they have also occurred in the Pacific Arctic, albeit at a much lower intensity (typically remaining below -15ºC) with much weaker impacts on the climate system.

Due to relatively slower variability in the Arctic atmospheric circulation and especially when stationay circulation pattern occurs, rare extremes can last long beyond daily scale, leading to an occurrence of rare monthly extremes. Thus, an increase in the frequency of daily SAT (**Fig. 2a, left**) is often coupled with a long-term increase in monthly SAT (**Fig 2a, right**) and midwinter SAT[7]. Pre-2000, events exceeding +1.0 and +1.5 standard deviations only occurred twice and once, respectively (**Fig. 2a, right**). However, a rare warm event centered over the North Atlantic Arctic in winter 2005/06 (when temperature anomalies of 12°C were observed in Longyearbyen, Svalbard[6]; **Supplementary Fig. 1a**; a regional average SAT increase reached 7.7ºC in Janauary 2006 from the winter (December-Feburary) seasonal mean climatology of -16.3ºC to -8.6ºC) seems to mark a transition of the climate state. Indeed, post-2000, 24 events and 10 events exceeded +1.0 and +1.5 standard deviations, respectively (**Fig. 2a, right**). The latter include events in: February 2012, showing a North Atlantic Arctic regional average SAT increase of 7.4ºC from the seasonal climatology to -8.9ºC; January 2016, an increase of 6.9ºC to -9.4ºC. This event is also recorded as the warmest winter for the pan-Arctic since observations began[43,44], featuring regional anomalies >4.0°C[8]; and February 2024, an increase of 5.3ºC to -10.1ºC.

With a substantial increase in daily and monthly rare warm events, there has come a corresponding decrease in rare cold events. For example, the maximum probability of rare cold daily SAT extremes decreases since the turn of the 21st century from 6.7% to 1.0% when using the -1.5 statendand deviation for 1979-1999 as the threshold (**Fig. 2a, left**). Likewise, the monthly cold events have also decreased in frequency and amplitude. Pre-2000, 23 and 5 events occurred ≤-1.0 and ≤-1.5 standard deviations, respectively, but post-2000, these reduced to 5 and 0 events (**Fig. 2a, right**).

[H3] Precipitation

Changes in rare precipitation extremes have also been observed over the North Atlantic Arctic. Any such precipitation changes are closely connected to rising temperatures through atmospheric moisture content, as dictated by the Clausius-Clapeyron relation and revealed by observations[14,45–47]—the maximum amount of water vapor the air can hold as a function of temperature. Thus, like SAT, the PDF of daily precipitation has shifted to higher magnitudes between 1980-2000 and 2000-2024 (**Fig. 2b, left**). Specifically, the maximum probability of rare heavy events increases from 7.4% to 11.1% using the +1.5 standard deviation as the threshold (**Table 1**). Two rare heavy precipitation events occurred in Ny-Ålesund, Svalbard in winter 2012 (**Supplementary Fig. 1b**), with 98.0 mm falling on 30 January (25% of annual mean precipitation) and 272.0 mm from 26 January - 9 February (70% of annual mean precipitation)[16]. Similar to the extreme warm events, extreme precipitation events over the North Pacific Arctic have occurred at a much weaker intensity than observed in the North Atlantic Arctic owing to a predomiant influence of the climatological Beautfort High in this area[48,49], where cyclone activity, a major precipitation driver, is much lower than that over the North Atlantic Arctic[49,50].

Daily events also translate into rare monthly totals. Monthly precipitation exhibits a statistically significant positive long-term trend, reaching 0.08 mm day^{-1} dec^{-1} (**Fig. 2b, right**). Likewise, an increasing number of climatologically rare events is apparent pre- and post-2000 (**Fig. 2b, right**); events ≥1.0 and ≥1.5 standard

deviations were observed 4 and 1 times pre-2000, and 16 and 10 times post-2000. Consistent with the rare extreme warm event, a rare heavy precipitation also occurred in Januanry 2006 with an increase of 0.53 mm day^{-1} from the winter (December-Feburary) seasonal mean climatology of 1.20 mm day^{-1} to 1.74 mm day^{-1}. The first two strongest events occurred in January 2017 and December 2018, showing an increase in preciptiaion of 1.04 mm day^{-1} and 0.80 mm/day^{-1} to 2.24 mm day^{-1} and 2.00 mm day^{-1}, respectively. Note that the relatively smaller magnitude in precipitation increase than SAT can be attributable to two factors: 1. The statistics includes all days, while precipitation does not occur every day; and 2. rare extremes always occur for a few hours, which can be masked by the daily average.

In addition to the amount of precipitation, extreme changes are apparent in its phase. Warming is associated with extreme rain-on-snow events. For example, summer rainfall was observed for the first time in the modern record on 14 August 2021 at Summit (at an elevation of 3200 m) on the top of the GrIS[17]. Rare rain-on-snow events are also increasing in Svalbard[18,20], mainly showing a step change around 2000, consistent with the rate warm and heavy precipitation events. However, the findings are uncertain due to a lack of sufficient in-situ observations[19].

[H3] Wind

Rare extreme winds have similarly been observed and appear to follow an increasing trajectory. Quantifying such changes is generally challenged by a lack of in-situ observations, especially at high temporal and spatial resolutions. Nevertheless, analyses suggest the frequency and magnitude of monthly extreme winds (defined as daily windspeed greater than the 95th percentile in each month) has increased in the North Pacific Arctic throughout the year (at the maximum rate of 2.6% dec^{-1} in October) and from July-November (at the maximum rate of 1.13 m s^{-1} dec^{-1} in October), respectively[21]. Anecdotal evidence of individual events also hints at more rare wind extremes post-2000 compared to pre-2000. Indeed, pre-2000, an extreme windspeed of 32.6 m/s was measured on 12 January 1993 at Bear Island, Svalbard[51], but other examples are limited. Post-2000, however, suggests more extreme winds occurred, including: windspeeds exceeding 25 m/s between 21 and 26 February 2018 in northeast Greenland[22], the highest windspeed at this station since 1961; a strong wind event exceeding 20 m/s in the Beaufort Sea around 9 March 2013[23]; and a record high wind speed reaching 28 m/s over the Barents Sea over the Barents Sea on 24 Januanry 2022[52]. Of course, such anecdotal evidence will be heavily biased by limited observations and a systematic evaluation and so should not be taken as evidence of robust increases.

[H2] Ocean.

[H3] Poleward ocean heat transport

One of the most pronounced rare extreme oceanic events are pulses of intense poleward North Atlantic heat transport into the Arctic. While transport of Atlantic water through the Fram Strait and the Barents Sea into the Arctic is a climatological feature, the magnitude of this inflow is increasing, reflecting more frequent and intense pulses. Comparing 1993-2000 and 2000-2017 (the time periods selected on the basis of data availability indicates marked shifts in both the mean state and extremes between the two periods (**Fig. 2c, left**). The extreme end of the distribution during the latter period is outside the range of the earlier period, suggesting an increased likelihood of extreme heat transport events after 2000/01. Indeed, the maximum probability of rare extreme transport events increases from 6.7% to 16.1% when using the +1.5 standard deviation as the threshold (**Table 1**).

A time series of heat transport provides additional evidence of these changes. A statistically significant increasing trend is obvious from 1993-2016, reaching 0.60 TW dec^{-1} (**Fig. 2c, right**). Clearly evident, however, are strong pulses of intense poleard transport. Post-2000, there are 6 instances of events ≥1.5 standard deviations (Oct 2005, Nov 2011 and Dec 2015), as well as 11 further events ≥1.0 standard deviations (**Fig. 2c, right**). Pre-2000, only 1 event ≥1.0 standard deviation occurred. The first event in winter

2005/06 witnessed unprecedented extreme heat transport, reaching 379.7 TW (about 67.0 TW above the climatological mean of 312.7 TW) and exceeding +2.0 standard deviations of its variability[6,26,53]. Following this event, several instances of similarly anomalously large heat transport occurred in the following years[26]. Indeed, the extreme transport reached to 381.3 TW in winter 2011/12 and 378.2 TW in winter 2015, respectively.

Although weaker than the Atlantic, poleward North Pacific Ocean heat transport through the Bering Strait has also increased, including three extremely high pulses in 2007, 2017 and 2018, reaching about 19 TW in annual mean and almost doubling the mean value during the prior years[27].

[H3] Atlantic layer temperature

Accompanying increased heat transport into the Arctic are temperature anomalies and shoaling of the Atlantic water layer[28]. Like other variables, a distinct shift is evident in the distribution of winter Atlantic water layer temperatures (at 200 - 600 m depth). The mean climate state during 2000-2023 becomes much warmer, reaching the extreme end of the distribution seen during 1980-2000 (**Fig. 2d, left**). The extreme tail of the latter period also exceeds the range of variability of the earlier period, highlighting increased probably of extremes (**Fig. 2d, left**). For example, between 1980-2000 and 2000-2023, the maximum probability of extreme occurrence increases from 6.7% to 83.3% when using the +1.5 standard deviation as the threshold (**Table 1**). This suggests that low probability, rare exteme events identified during the earlier period become more frequently occurred during the latter period.

Various high magnitude warming events are also observed, corresponding to the shift in PDF. Post-2000, 1 event and 9 events ≥1.5 and ≥1.0 standard deviations occurred, respectively, whereas no such exceedances occurred pre-2000 (**Fig. 2d, right**). Of these occurrences, the extreme event in 2006/07 shows an increase of temperautre by 1.5°C from the seasonal mean climatology of 8.6°C to 10.1°C. The time of this event is highly consistent with that for SAT, precipitation, and the poleward North Atlantic warm water transport. Following this event, similar magnitude of events consecutively occurred in 2015/16, 2016/17, and 2018/19 with a temperautre increase to 10.0°C, 10.6°C, and 10.3°C, respectively. Accordingly, Atlantic layer temperature in the Arctic exhibits a positive trend of 0.49°C dec^{-1} (**Fig. 2d, right**).

[H3] Mixed layer and sea surface temperature

In addition to lateral heat transport and associated warm events, rare extremes have been observed in mixed layer temperature. In the Central Arctic, mixed layer temperature distributions have shifted substantially to the right, such that the dominant part of the distribution in 2000-2023 is largely outside the range observed during 1979-1999 (**Supplementary Fig. 2a**). As with other variables, this shift indicates a much-warmed climate mean state and an increased probability of extreme events. Specifically, the maximum probability of rare event identified using the +1.5 standard deviation for 1979-1999 increases from 6.7% to 81.5% (**Table 1**). The same as the Atlantic layer temperautre, this suggests that rare event in the former period is no longer rare and further indicates a shift of the climate into a new state.

As a manifestation of this change, rare extreme warm mixed layer temperature events have occurred. From 1979-1999, there was no any events above the climatological mean from 1979-2023, but during 2000-2023, all events are in the positive range of variability above the climatology, including 4 and 7 that are ≥1.5 and ≥1.0 standard deviations (**Supplementary Fig. 2b**). The first substantial event occurred in summer 2007 when temperature increases by 4.0°C from the summer seasonal climatological mean of 1.0°C to 5.0°C. This event was intermittently followed by the same or more intense events in later years, notably in 2015, 2016 and 2023, with an increase of temperautre to 5.3°C, 6.9°C, and 7.3°C, respectively. Accordingly, the trend in summer mixed layer temperature reaches 0.53°C dec^{-1}, statistically significant at the 99.9% level of confidence based on a t-test (**Supplementary Fig. 2b**).

The distribution of SST anomalies in the summer open water and marginal ice zone areas also demonstrates the same shift as mixed layer temperature. Correspondingly, a series of unprecedented marine heat waves

have been observed at the surface, ascribed to extreme and earlier summer sea ice decrease events that increase ocean absorption of downward atmospheric and radiative energy with enhanced albedo feedback[10,54]. For instance, the maximum probability of rare marine heatwave events detected with the threshold of +1.5 standard deviation during 1982-1999 increases from 6.7% to 66.8% during 2000-2023 (**Supplementary Fig. 2c; Table 1**). The first of these extreme marine heatwave events occurred in August 2007, when SST increases to 10.2ºC from nearly 0ºC of summer (July-September) seasonal climatological mean. Other extreme marine heatwaves continuely occurred in September 2012, August 2019, and August 2023, with a SST anomaly increasing to 4.6ºC, 8.9ºC, and 7.2ºC, respectively. Thus, monthly maximum Arctic open water sea surface temperature has witnessed a statistically significant increase of 2.52℃ dec^{-1} (**Supplementary Fig. 2d**), consistent with other evidence of increasing intensity (maximum and mean SST anomaly), frequency, duration and areal coverage of marine heat waves since the mid/late 2000s[55]. These surface warm events can also translate to the deeper ocean, as evidenced by a near doubling of heat content of the Beaufort Gyre halocline based on the data analysis from 1987-2017[56].

[H2] Cryosphere.

[H3] Sea ice extent

Arctic sea ice change is characterized by rapid and exteme reductions in sea ice extent[70]. The PDF of September sea ice extent loss relative to the climatological sea ice extent maximum for 2000-2023 is largely outside the range observed for 1979-1999, indicating increased probability of rare extreme ice loss during the latter period (**Fig. 2e, left**). In particular, when using -1.5 standard deviation as the threshold, the maximum probability of extreme sea ice extent loss event identified during 1979-1999 increases from 6.7% to 90.2% during 2000-2023. This suggests that the extreme low sea ice extent events below -1.5 standard deviation of the sea ice extent variability and changes during the former period become more frequent. September ice extent loss, in turn, exhibits a statistically significant negative trend, reaching -0.88 x 10^6 km^2 dec^{-1} (**Fig. 2e, right**). The largest decreases mainly occurred in the Pacific Arctic and Eurasian sector.

These changes are further evidenced by specific extreme ice loss events. 12 Septembers experienced extreme ice loss ≤-1.0 standard deviation relative to the climatological mean sea ice extent loss of 1.9 x 10^6 km^2 from 2000-2023, including 4 months ≤-1.5 standard deviations; by comparison, 11 Septembers were ≤-1.0 standard deviations in 1979-1999 (**Fig. 2e, right**). The strongest loss events occurred in 2007, 2012, 2020 and 2023 comapred to the climatological maximum of sea ice extent of 8.26 x 10^6 km^2, accordingly leading to minimum ice extent in these years[6,11,13,57,58]. In 2007, sea ice extent loss was 3.76 x 10^6 km^2. Following this event, a number of rare sea ice extent loss events continually occurred, including: 2012, 2020, and 2023, showing a sea ice extent loss of 4.52 x 10^6 km^2, 4.14 x 10^6 km^2, and 3.72 x 10^6 km^2, respectively.

While summertime ice loss dominates, rare extreme sea ice loss events have also occurred in winter. Corresponding to the areas of extreme atmospheric warm events, these wintertime sea ice loss events largely occur in the Barents Sea[59,60], where there is a sea ice extent delicing trend of -0.78 x 10^5 km^2 dec^{-1}. Preceding the rare extreme event in September 2007, a rare extreme sea ice extent loss of 0.58 x 10^6 km^2 (relative to the climatological maximum of 0.88 x 10^6 km^2) occurred in March 2007. Afterwards, rare extreme loss of 0.64 x 10^6 km^2 and 0.68 x 10^6 km^2 continully occurred in the Marches of 2012 and 2016. In addition, an extreme sea ice thinning event was observed in Fram Strait 2007, being consistent with a reduction of basin-wide multiyear ice fractions[61], triggering a step change from a thicker and deformed sea ice regime to a thinner and more uniform sea ice regime[62], and resulting in a decreased ice export with a record minimum in 2018[63].

Extreme ice loss has also occurred at daily timescales, often associated with intense weather systems such as cyclones, anticyclones and atmospheric rivers. Once such rapid ice loss event occurred in August 2012 where

a super Arctic cyclone decrease ice extent by ~0.9 million km^2 over 7 days[64]. Likewise, a cyclone in August 2016 resulted in ~0.26 million km^2 of ice loss within the northern Chukchi and Beaufort seas alone over a 9-day period, a loss rate six times the climatological mean[13]. During 1989-2019 winters, ~25 extreme sea ice loss events (using a criterion of consecutive 5-day sea ice concentration anomalies below -1.0 standard deviation) occurred in the Barents and Kara seas[65]. Another manifestation of extreme daily scale sea ice extent loss event is the occurrence of large winter polynya in climatologically old and thick icepack. For example, an unprecedented large winter polynya with an area more than 60000 km^2 occurred off the north coast of Greenland from 14 February - 8 March 2018[22,66,67]; and a similar polynya event with an area exceeding 3000 km^2 was observed on 13-28 May 2020[82]. Although theses winter events favors increasing sea ice mass, they suggest a substantially thinning of the sea ice thickness in this area, increasing vulnerablity and mobility of the perennial sea ice in response to atmospheric forcing.

[H3] Greenland Ice Sheet melt

The GrIS has also experienced negative mass balance trends over the satellite era[70,71], part of which can be attributed to surface melt events. Marked shifts are evident in the distribution of summer GrIS melt extent between 1979-1999 and 2000-2024, with an increase in maximum probability of rare extreme melt events from 6.7% to 69.6%, when using the +1.5 standard deviation from 1979-1999 (**Fig. 2f, left**). Like sea ice, the distributions of summer seasonal maximum GrIS melt extent during the latter period is, thus, largely outside the range observed during the earlier period. Accordingly, all summers witnessed melt extent ≤0.5 standard deviations or below the climatological mean over 1979-1999, respectively, whereas 3 and 6 summers experienced melt extent ≥1.5 standard deviation and ≥1.0 standard deviations, respectively (**Fig. 2f, right**). Accompanying the PDF shift is a corresponding increasing trend in melt extent of 0.08 x 10^6 km^2 dec^{-1} (**Fig. 2f, right**).

Several notable extreme summer monthly maximum GrIS melt events have contributed to these changing characteristics[72,73]. An extremely large melt event occurred in July 2005, which shows an increase of the melt extent by 0.19 x 10^6 km^2 from the summer climatological mean of 0.29 x 10^6 km^2 to 0.48 x 10^6 km^2. July 2012 was also characterized by record high and widespread melt[31,74], consistent with record high SAT at Summit[75]. In this month, the melt extent increased to 0.72 x 10^6 km^2. Melt occurred across 96% of the GrIS on 12 July 2012, including the dry snow facies around Summit Station where melt previously occurred in 1889[75]. In July 2023, the melt extent reached to 0.6 x 10^6 km^2, which is the second record high since 1979.

GrIS melt extent shows large variability temporally and spatially, leading to different form of extremes. The summation of daily melt extent anomalies over the extire summer from June-August 2007 was extremely higher than previous years[30], the magnitude of which was about 80 x 10^3 km^2 abve the mean value from 1973-2008, ~60% larger than the notable event of 1998. An extremely long melt duration occurred in summer 2019, about 40 days above the 1981-2010 climatolgical mean[76]. Coincident with the first-observed rainfall at Summit on 14 August 2021, extreme surface ablation caused the bare-ice area to reach a near-record-high value, with the snowline moving up by 788±98 meters[17]. In addition, an unprecedentedly late September melt event occurred in 2022, which affected 36% of the ice-sheet surface and represents an extension of the Greenland melt season under a warming climate[77].

[H1] Driving mechanisms of Arctic extremes

A unifying aspect of observational changes in Arctic rare extremes is a systematic increase in their frequency and intensity starting from the turn of the 21st century, marked by a consistent occurence of striking extreme events ~2005-2008 across the atmosphere, ocean and cryosphere. This consistent step change supports the idea of a transition of the Arctic climate system into a new (mean) state[6,63,78]. The driving processes of these extremes and their changes are now discussed (**Fig. 3**), framing around a 'pushing and triggering' mechanism: anthropogenic warming destabilizes the climate system and 'pushes' it to a more susceptible

state, in turn, facilitating the occurrence of extreme events through subsequent 'triggers' (including large-scale and synoptic scale atmosphere-ocean-ice processes). Nonlinear interactive processes involved in the 'pushing and triggering' mechanism would create a strengthened impetus to drive the Arctic climate system to cross a threshold or a tipping point to the new state[79–83].

[H2] Pushing mechanisms

Destabilization of the Arctic climate system driven by anthropogenic warming acts as the 'pushing' mechanism. In the Arctic (>60°N), annual mean SAT shows an increasing trend of 0.63ºC dec^{-1} from 1979-2023, a rate 3.5 times the global mean[2–5,84] (**Supplementary Fig. 3**). Accompanying this long-term trend, a step change is also evident before and after the turn of the 21st century, indicating an elevation of climatological mean SAT by 1.48 ±0.09°C in 2000-2023 relative to 1979-1999. Winter warming trend is even more pronounced at 0.68ºC dec^{-1} (4.2x the global mean), while summer warming trend is slightly lower at 0.37ºC dec^{-1} (1.8x the global mean). Associated with these trends, the climatological mean SAT was also elevated by 1.70 ±0.16°C and 0.87 ±0.08°C for 2000-2023 from 1979-1999, respectively. This large temperature change compared to the rest of the globe describes Arctic Amplification, largely driven by complex feedback processes, including ice/snow-albedo, lapse rate, Planck, and water vapor and cloud feedbacks that exacerbate temperature responses[33,85–89].

Long-term, amplified warming increases the sensitivity and reduces the resilience of the Arctic climate system. As a consequence, "the 'pushing' mechanism preconditions the occurrence of extreme. For example, the elevated baseline SATs and SSTs increase probability of SAT and SST to exceed their long-term variability range, causing an extreme event, even if the specific driver were the same as during the pre-AA era. Similarly, sea ice and ice sheet temperatures become closer to their melting points, allowing easier melt under the same amount of heat energy input; thinner ice also becomes more vulnerable to energy budget perturbations than in the previous climate state. Accordingly, accelerated sea ice loss (54,300±2,700 km^2 yr^{-1} in annual mean from 1979-2021[70]) and GrIS mass loss (169 Gt yr^{-1} from 1992-2020[90]) have been observed, including marked extremes (**Fig. 2**).

[H2] Triggering mechanisms

While Arctic warmig pushes the system to a state in which extremes are more likely, multiscale climate system variability due to non-linear atmospheric-ocean-sea ice interactions 'triggers' the extreme events themselves and the state shift[91]. These multi-scale triggers include large scale atmosphere-ocean-ice variability (such as modes of atmospheric variability), as well as synoptic or mesocale dynamics (such as cyclones). These aspects are now discussed.

[H2] Large-scale coupled variability

Large-scale variability can both drive the occurrence of seasonal scale extremes and precondition the genesis or development of synoptic or mesoscale systems to cause daily scale extremes[92]. Modes of coupled atmospheric variability are one such contributor, providing favorable dynamic settings for rare extremes and causing energy imbalances through modified poleward heat and moisture transport in the atmosphere and heat transport in the ocean. The Arctic Oscillation (AO) and the Arctic Rapid change Pattern (ARP) are two such fundamental and important modes.

The AO (or the North Atlantic counterpart, the North Atlantic Oscillation, NAO) is an important driver and preconditioner of Arctic extremes. The AO is the leading mode of winter atmospheric circulation variability in the Northern Hemisphere[93,94], describing the coordinated temporal variability of the Icelandic Low, Azores High and Aleutian Low from their long-term climatology (**Supplementary Fig. 4)**. Thus, fluctuations of the AO/NAO modulate large-scale wind patterns and, accordingly, heat and moisture transport and extreme event

occurrence. For example, a positive NAO regime is associated with higher-than-normal probability of extreme warm days over the Norwegian Sea and Scandinavia, while a negative NAO regime is associated with higher-than-normal probability of extreme warm days over Baffin Bay and large parts of the Canadian Archipelago[95–97]. The positive AO regime from the 1980s to the mid 1990s would have therefore contributed toward increased Arctic winter SAT and decreased sea ice extent[98,99], but the AO is generally neutrual or in negative AO regime thereafter[6,100,101] suggests a minimal direct triggering role of Arctic extremes post-2000. Indeed, post-2000 extreme warm events were observed over the Atlantic Arctic[6–8,44] (**Fig. 2b; Supplementary Fig. 1a)**, a region without statistically significant SAT-AO relationships (**Supplementary Fig. 4a).** Nevertheless, the positive AO from the 1980s to 1990s caused notablely larger warming and sea ice decrease than before, which increased vulnerability of the Arctic climate system and could have preconditioned the increased extremes post-2000.

While the AO is not directly connected to the post-2000 increase in Arctic extremes, the same cannot be said for the Arctic Rapid change Pattern (ARP)[6]. The ARP is expressed as a monthly sea level pressure seesaw between the Siberian high and the Aleutian low (**Supplementary Fig. 4**). The negative ARP is characterized by a strengthened and northwestward-expanded Siberian High, an intensified Aleutian Low and a weakened Beaufort High (**Supplementary Fig. 3e**). This pattern causes meridionally aligned wind blowing from the North Atlantic or the North Pacific to the central Arctic that strongly influences SAT in the Atlantic Arctic **(Supplementary Fig. 4d)** via steering atmospheric heat and moisture transport and oceanic heat transport[6,14] (**Supplementary Fig. 5**); warm and moist airmass increases downward turbulent heat fluxes, cloud formation and downward longwave radiation[102,103], contributing to SAT, precipitation and sea ice extremes. These ARP-extreme connections are strengthened after winter 2001/2002, with the three record-breaking North Atlantic Arctic winter extreme warm events (January 2006, Juanary-Feburary 2012 and January 2016) and the pan-Arctic record-breaking sea ice minimum event (September 2007) coinciding with ARP index values that exceed -/+1.5 standard deviations. A substantial shift toward extreme negative ARP post-2000 (**Supplementary Fig. 4d**)[6] could therefore have caused increased occurrence of warm SAT (and related) extremes in the North Atlantic Arctic. The ARP itself is thought to be a consequence of the interplay between anthropogenic forcing and internal variability from changing sea ice[32] (as well as amplified jet streams through enhanced land-ocean thermal contrasts[50,104]), suggesting the importance of anthropogenically intensified interactions between the climate system components. Anthropogenically changed sea ice, ocean, and land conditions cause a formation of ARP and, in turn, the ARP feeds back to amplify the changes in the underlying sea ice, ocean, and land to trigger extreme events.

Other modes of variability might also come into play. These include the Barents Sea Oscillation and Arctic Dipole pattern[105,106], and teleconnections associated with the El Nino-Southern Oscillation[107–109], Pacific Decadal Oscillation[110,111] and Atlantic Multidecadal Oscillation[112–114]. The contributions of these modes to the increased frequency of the rare extreme warm events are not as prominent as the ARP. The Barents Sea Oscillation and Arctic Dipole pattern, for example, do not exhibit extreme values during extreme warm events in the North Atlantic Arctic (**Supplementary Table 1**) as neither support enhanced atmospheric heat and moisture transport and oceanic heat transport[115] from the North Atlantic or the North Pacific into the Arctic. Tropical and extratropical teleconnections also cause the largest SAT anomalies over the sub-Arctic and midlatitudes, but with limited atmospheric and oceanic heat transport directly affecting SAT in the central Arctic, especially the observed extreme warm events in the North Atlantic Arctic, and poleward ocean heat transport (**Supplementary Figs. 6-8**).

Troposphere-stratosphere interactions are a further driving force for atmospheric circulation anomalies and and extreme events. Sea ice retreat and ocean warming can trigger upward planetary Rossby wave activity flux that decelerates the polar jet stream and disrupts the stratospheric polar vortex[116]. These processes can cause Sudden Stratospheric Warming events and, in turn, weaken the stratospheric polar vortex[34]. A weakening trend of the stratospheric polar vortex has shown to be linked to an increased occurrence of sudden stratospheric warming events from 1980-2016[117,118]. The signals of the weakened stratospheric polar vortex propagate downward to influence tropospheric and surface circulations, manifesting as the regime transition of the AO and ARP from positive to negative[6,35,119]. The changed circulations are linked to the occurrence of blocking circulation patterns that drive Arctic heat waves, cold spells, extreme winds and

unprecedented polynyas. For exmaple, a rare extreme warm event in January-Feburary 2016 occurred when a split stratospheric polar vortex occurred[8]; an unprecedented large polyanya in climatologically thick ice off the north coast of Greenland from 14 Feburary-8 March 2018 due to anomalously warm southerly winds associated with a sudden stratospheric warming event[22]; an unprecendented winter anticyclonic winds driving sea ice from the central Arctic to the warmer Beaufort Sea follwoing a sudden stratospheric warming event beginning on 5 January 2021[24]; and a cold extreme over Scandinavia after a sudden stratospheric warming event in Feburary 2018[119]. Also, a shift of the stratospheric polar vortex to Greenland due to its weakening since 1985/86 steers strong cyclones to propagate into the Arctic[50], which is one of critical drivers triggering Arctic extremes. Considering that the stratosphere evolves more slowly than the troposphere, the disturbed stratospheric polar vortex can act as a source of predictability for major weather and climate events at lead times longer than two weeks[120,121]. In addition to the importance of stratosphere-troposhere interactions for triggering individule Arctic extremes, an increase in the frequency of sudden stratospheric warming events (Fig. 1 in ref[117]) might augment evidence supporting the Arctic climate system state shift since the beginning of the century.

While the modes of climate variability and stratosphere-troposphere interactions are key triggers of Arctic extremes via modulating heat and moisture transport, large-scale ocean circulation variability could also be important for driving poleward ocean heat transport. In the North Atlantic Arctic, heat transport can be linked with the Atlantic Meridional Overturning Circulation (AMOC). Here, AMOC-related anomalies in ocean temperature have been tracked all the way from the subpolar North Atlantic into the Barents Sea[53,122,123]. However, observed enhanced ocean heat transport into the Arctic disagrees with an apparent weakening of the AMOC[124,125], complicating understanding of AMOC connections to Arctic extremes. Nevertheless, the coincidence of extreme ocean heat transport events with extreme SAT events [at 1-3 months lead; **Fig. 2a (right) vs. c (right**)] does demonstrate their importance in general.

These large-scale drivers are naturally coupled and act to precondition chain reaction of extremes occurrence across the Arctic climate system through feedback processes once an extreme event occurs in one system component. For example, atmospheric circulation changes cause enhanced wind stress from the North Atlantic or North Pacific toward the central Arctic Ocean[6,27,53], dynamically forcing a increase in poleward ocean currents, heat transport (**Supplementary Figs. 9a, b**)[6,26,27,57], deeper layer warming[28] and ocean mixing increase[63], leading to extreme ocean events. These processes, in turn, contribute to ocean feedbacks to the overlying sea ice and atmosphere, preconditioning the occurrence and intensification of rapid sea ice loss or extreme atmospheric warm events through increased upward heat flux. Similarly, large-scale sea ice loss also initiates various feedbacks processes that drive sea ice, SAT or ocean extremes[54–56,127]. For instance, decreased ice cover and thickness reduces insulation effects, exposes more open water to direct atmospheric and radiative forcing[128,129], strengthens albedo feedbacks[130], increases free ice drift[131], and therefore enhances atmosphere-ocean-sea ice interactions, all of which would then impact fall freeze-up[56,132], preconditioning winter extremes to occur. Due to the chain reaction and strengthened feedbacks, the frequence of extremes consistently occur and increase across the Arctic climate system components, resulting in a step change for the system into a new state. These large-scale, systematic changes make the system more sensitive and susceptible to external forcing and internal dynamic disturbances, preconditioning more extreme occurrences subject to synoptic and mesoscale dynamic triggers.

[H3] Synoptic and mesoscale dynamics.

Synoptic and mesoscale weather systems can also trigger daily-scale extreme events. These systems include cyclones, blocking highs, polar lows and atmospheric rivers. The occurrence and intensity of these systems is predominantly preconditioned and driven by aforementioned large-scale atmosphere-ocean-sea ice system processes. The shift of the large-scale baseline climate state can also systematically increase the frequence of intense synoptic and mesoscale systems, contributing to increased likelihood of Arctic extremes.

Through their (thermos)dynamic processes[133–137] and related feedbacks with the underlying sea ice and ocean[13,138,139], cyclones are a dominant driver of Arctic extremes. Many such examples exist: in 2012, record low summer sea ice extent[11,140] is linked to a super cyclone in August; in 2016, extreme winter warm events are linked to a cyclone in January[9], and low summer sea ice extent to an intense cyclone in August (**Supplementary Fig. 10a, b**)[13]; in 2018, the unprecedented winter North Greenland polynya is linked to a strong cyclone in late February and early March[47,154]; and in 2022, weekly record sea ice loss in the Barents-Kara Seas to a cyclone in January[52]. Such strong summer cyclones are initially generated and intensified by baroclinic instability, and then intenfied and maintained by the downward intrusion of the summer lower Stratospheric Arctic Vortex[140,142–145] (or the Tropopause Polar Vortex when presented at the tropopause[146]) (**Supplementary Fig. 10c**). An observed intensification of the Arctic lower tropospheric baroclinicity and the strengthened summer lower stratospheric Arctic vortex[50] have contributed to the long-term intensification of Arctic cyclones[49,50,133]. Winter Arctic cyclones have also intensified, which are predominantly driven by lower troposperhic baroclinic instability and a sourthward shifted winter planetary stratospheric polar vortex to Greenland due to a weakening of the stratospheric polar vortex[50].

Blocking highs can also tigger extreme events, describing stationary or slow-moving high pressure weather systems. Owing to their stationary or slow-moving nature, blocking highs favor persistent gain or loss of heat energy through radiative and meridional airmass transport processes. Winter Scandinavia/Ural blockings increase poleward atmospheric heat transport, leading to extreme warm days in the North Atlantic Arctic (**Supplementary Fig. 10d**)[95–97]. Summer Greenland blockings, for instance, transport relatively warm air to the western flank of the GrIS and form a heat dome over Greenland, causing extreme ice sheet surface melt[73,75]. Such processes are responsible for extreme GrIS melt events in summer 2012[75] (**Fig. 2f**). Moreover, an unusually persistent blocking high in summer 2019 caused exceptional peak warmth and melt at an unusually late time in the melt season[76,147]. The frequency of summer Greenland blocking highs at the surface and mid-troposphere has increased over time, suggesting an increased occurrence of extreme warm events and resultant ice sheet surface melt that can accelerate the GrIS mass loss.

Synoptic scale cyclones or blocking highs (or their co-occurrence) can further enhance poleward moisture transport, forming Arctic atmospheric rivers. Atmospheric rivers represent extremes in synoptic scale atmospheric moisture transport. Accordingly, they dramatically increase atmospheric water content and cloudiness, thereby initiating interactive processes—and extreme events—across the atmosphere, ocean and sea ice[9,141,148,149,150]. Atmospheric rivers have, thus, been implicated in several Arctic extremes, including: an entire GrIS surface melt for the first time over a century in July 2012 (**Supplementary Figs. 10e**)[151]; an extreme sea ice extent loss events in August 2012 and July 2020[152]; an extreme winter warm event in December 2015[153]; and unprecedented rainfall at the GrIS Summit on 14 August 2021[17]. Physical processes associated with atmosheric rivers include enhanced water vapor greenhose effect, cloud-forced downward longwave radiation, and turbulent heat fluxes[29,65,154]. The frequency of winter atmospheric rivers into the Barents-Kara Seas increased from 1979-2021 (**Supplementary Figs. 10f**)[65,154], perhaps contributing to the increased probability of extremes in this area.

Intense mesoscale cyclones, polar lows, could also be linked to Arctic extremes. Polar lows occur in maritime cold air outbreaks in higher latitudes, their lifetime typically ranging from a few hours to a couple of days[155]. As their tracks are seldom poleward, their role in generating Arctic extremes is not comparable to synoptic-scale weather systems. However, owing to their rapid intensification and large evaporation, polar lows commonly bring gale force winds and extreme snowfall[156].

Like large-scale variability, these synoptic processes will also excite feedback processes that intensify extreme events and precondition the system for further events. For instance, strong winds driven by the co-

occurrence of a cyclone and a blocking high can blow surface snow to the atmosphere, increasing floating snow sublimation, atmospheric water vapor and low level clouds[141]. Furthemore, sea salt aerosols from blowing snow increase longwave emissivity of clouds, enhancing downward longwave radiation to intensify extreme warm events[157]. When this snow-blowing process is combined with a polynya, an increased thermal contrast across the edge of the polynya, in turn, accentuates surface winds, enlarging the polynya or maintaining it for a longer[141]. In addition to its enhancement to sea ice-albedo feedback, intense cyclones can also intensify atmosphere-ocean-sea ice interactions through increasing upper ocean mixing, deeper layer warm water upwelling, and, in turn, upperward oceanic heat flux. All of these changes decreases sea ice and adds more heat energy to the atmosphere, fueling cyclone intensification[13,138]. Further, cyclone-induced increase in water vapor and atmosperhic rivers enhance water vapor-radaition and cloud-radiation feedbacks initiated by large-scale processes.

Intense synoptic and mesoscale weather systems represent extremely intensified atmosperhic circulation perturbation, adding additional strength to the dynamics trigger to initiate extreme events under and following large-scale preconditioning effects. They substantially strengthen interactions and feedbacks between the atmosphere, ocean, and sea ice. They strengthen atmospheric moisture transport, cloud-forcing feedback and downward longwave radaiton, and increase ocean mixing, deeper ocean heat release, and turbulent heat fluxes between the atmosphere, ocean, and sea ice. All of these works together to drive development and sustaintance of extreme events.

Anthropogenic warming, large-scale coupled dynamics, and synoptic-mesoscale weather system synergically form the 'pushing and triggering' mechanism. The long-term anthropogenc forcing destbilishes the Arctic climate system to push it to become vulnerable. Radical changes in the large-scale atmospehric circualtion and its interaction with the underlying ocean and sea ice triggered a mean climate state shift ~2000 and increased occurrence of extreme clusters ~2005-2008 due to chain reaction and cascading effects across the system components. The fommer two drivers also precondition increased frequency and intensity of synoptic and mesoscale weather systems to trigger more extremes to occur.

[H1] Projections of Arctic extremes

Ongoing anthropogenic warming is expected in the future[158,159]. The baselines of Arctic Earth System components are, therefore, set to be pushed even further beyond their natural limits[158–162]. In such cases, a new climate state emerges, triggering extreme events more easily under the 'pushing' effect (**Fig. 3b**). These new climate states can be assessed using the Time of Emergence[163] (ToE)—the year when the decadal mean of a selected climate variable or indicator exceeds its value in the reference decade by 2.0 standard deviations.

Corresponding changes to extreme event drivers themselves also facilitate extremes. These include: a more frequent occurrence of positive winter AO (or NAO)[164], favoring pan-Arctic warming[98,99]; a more frequent occurrence of the ARP and, in turn, extreme warm events in the North Atlantic Arctic atmosphere and Atlantic water layer due to enhanced poleward heat and moisture transport[32]; suspected increases in the frequency, intensity and longevity of cyclones, albeit with uncertainty and regional dependence[165–169]; strengthened intensity of Arctic atmospheric rivers, especially in the summer[170]; and a northward shift in polar lows[171–174]. Like in observations, shifts in the likelihood of extremes can also be assessed by comparing PDFs in historical and future climate model simulations.

Ongoing changes in Arctic extremes are now discussed, examining the ToE (**Fig. 4**) and extreme event occurrence (**Fig. 5**) for SAT, precipitation, ocean temperure, sea ice extent and GrIS melt. Simulations and projections with the Community Earth System Model (CESM) Large Ensemble Project (LENS)[175], CMIP6[176] and a coupled atmosphere-ocean-ice-sheet model[177] are used. CESM-LENS is forced with RCP8.5 scenario

and all other models with SSP5-8.5 scenario to clearly identify and elucidate the effects of the projected future greenhouse gas emissions forcing.

[H2] Atmosphere

[H3] Temperature

Large changes in Arctic SAT have already occurred and are expected to continue in the future. Indeed, February SAT is already throught to be outside the range of historical variability across a large area of the Arctic spanning the Canadian Archipelago to the East Siberian Sea, as suggested by a ToE of ~2025 (**Fig. 4a, left**). Elsewhere, ToE occurs ~2040-2075 depending on the location (**Fig. 4a, left**). North of Svalbard, for example, ToE is ~2070 (**Fig. 4a, right**), the delayed occurrence linked to high SAT variability related to the sea ice edge. These patterns are pretty consistent across other winter months, although the ToE is later than suggested by observations[6,78,83].

These shifts in the base variability of SAT make the system more susceptible to extreme events. The CMIP6 multi-model ensemble individates clear shifts in the probability distribution of winter SAT over the course of the 21st century in the North Atlantic Arctic (**Fig. 5a, left**), where the frequency of observed extremes significantly increased (**Fig. 2**). In particular, the mean state from 2069/70 - 2098/99 falls into the extreme end of the distribution during 2014/15 - 2044/45, substantially increasing the probability of extreme warm events. Indeed, when using the +1.5 standard devidation from 1984/85-2013/14 as the threshold for identifying rare extreme warm events, the maximum probability of extreme occurrence considerably increases from 6.7% during 1984/85-2013/14 to 23.55% in 2014/15-2044/45 and 79.3% in 2069/70-2098/99, respectively (**Fig. 5a, left; Table 1**). The occurrence of individual rare extreme events (SAT anomaly >+2.0 standard deviation) in each of the models with a moving 20-year time window, therefore, intensifies with the projected increase in global mean winter SAT, rising 3.07 °C °C^{-1} (**Fig. 5a, right**). These reported increases are consistent with other estimates, including suggestions that a 50-year return daily maximum warm event during 2071 - 2100 is about 5.7°C (3.2 - 9.2°C) warmer than during 1985-2014 and a 50-year return daily minimum cold event is 13.3°C warmer (9.6 - 17°C) under SSP5-8.5 (ref[178]).

[H3] Precipitation

As in observations, changes in temperature are closely accompanied by changes in precipitation, both in regards to the phase and the magnitude. For instance, warming causes seasonal phase changes from snow to rain, with rain becoming the dominant precipitation type in the future Arctic[179,180], likely mainly driven by intensified local evaporation from sea ice loss[181]. Such phase shifts reduce the length of the snow season. Changes above natural variability emerge earliest in the central Arctic in ~2030 (**Fig. 4b, left**), associated with a combination of a shortened snow season and extended rain season. ToE occurs later elsewhere in the Arctic (~2030-2070) owing to the high SAT variability (**Fig. 4a, left**) that influences cloud phase composition. Indeed, ToE of the first rain day in Svalbard is 2070 (**Fig. 4b, right**), consistent with the time when SAT signals emerge (**Fig. 4a, right**). Rain-on-snow events, as observed on the GrIS and in Svalbard[17,18], would thus be expected to increase in the future warming climate.

Accompanying new Arctic precipitation baselines are corresponding changes to the frequency and magnitude of extremes. In the North Atlantic Arctic, the mean climate states shift towards greater variability and increased precipitation (**Fig. 5b, left**), as also projected for seasonal-mean and annual-mean Arctic precipitation[180,182]. Specifically, the maximum probability of rare events identified during 1984/85-2013/14 using +1.5 standard deviation as the threshold increases from 6.7% to 17.3% during 2014/15-2044/45 and 55.8% during 2069/70-2098/99, recpectively (**Table 1**). The stronger the warming, the stronger precipitation anomalies will be, increasing 0.18 mm d^{-1} °C^{-1} with the projected global mean winter SAT for extreme (>2 standard deviation) monthly precipitation anomalies (**Fig. 5b, right**). Likewise, annual maximum one-day

precipitation and 5 consecutive precipitation is projected to be 39.5% (26.9 -54.6%) and 36.6% (22.3-57.8%) more intense in the future, respectively[178].

[H3] Wind

Arctic extreme surface winds are also projected to increase in the future. Any such changes are related to reduced surface roughness from sea ice loss, lower tropospheric stability from enhanced surface warming, and intensified cyclone activity[183,184]. Extreme 6-hourly surface winds (>95th percentile) could increase up to 100%, by 2071-2100 relative to 1971-2100 under RCP8.5 scenario[183]. The largest increases occur in autumn and winter over open water areas. Increased wind speeds over open water (in conjunction with sea ice loss), would consequently enhance ocean wave extremes. Indeed, in response to autumn cyclones, offshore annual maximum significant wave height increases up to 6 meters in 2081-2100 relative to 1975-2005 under RCP8.5, representing wave heights that are 2-3 times those of the base period[185,186]. The maximum increases occur in the open ocean, including northern portions of the Chukchi and Beaufort seas.

[H2] Ocean

Anthropogenic signals in Arctic summer SST occur much earlier than SAT and precipitation. A new decadal mean climate state emerged as early as the 1990s over the Eurasian Arctic Ocean as indicated by ToE (**Fig. 4c, left**), but slightly later (~2012) north of Svalbard because of the large fluctuations of thicker sea ice outflow through Fram Strait (**Fig. 4c, right**). In the rest of the central Arctic, ToE appears ~2050 except the perennial sea ice covered area (white color shadding), but all more southerly locations, including the Nordic Seas and Barents Sea, are expected to have shifted to a new state by ~2030 (**Fig. 4c, left**). In relation to other variables, these signals emerge earlier because of substantial sea ice retreat and resultant enhancement of albedo feedback, consistent with the larger changes of SST in the observations from 1982-2023 (**Supplementary Fig. 2c,d**). Because changes in SST is critically influenced by sea ice and there is a lack of albedo feedback during winter months, the state change of winter SST would be much later than summer.

As for other variables, new emergent ocean states translate to marked shifts in the PDF. Consistent with the much earlier occurrence of summer SST ToE, the upper ocean mixed layer temperautre shows pronounced shifts of its mean state, indicating an increase in the probability of rare extreme events (**Supplementary Fig. 11a**). With the same threshold of +1.5 standard deviation based on 1985-2014, the maximum probability of rare extreme occurrence increases from 6.7% to 28.5% for 2015-2044 and 83.2% for 2070-2099, respectively (**Table 1**). The temperautre anomaly of summer extreme events (>+1.5 standard deviation) increases with the projected global mean summer SAT anomaly at a rate of 0.98 ^{o}C $^{o}C^{-1}$(**Supplementary Fig. 11b**). At the end of the 21st century, the temperautre anomaly relative to the climatological baseline likely increased ~4.5^{o}C. This is comparable with the an estimate of ~3^{o}C for the entire Arctic Ocean and ~4^{o}C for the Barents Sea using SST[187].

For winter Atlantic layer temperature, for example, substantial changes are also evident (**Fig. 5c, left**), although the changes in this deeper layer is predominantly driven by the North Atlantic water inflow. The PDF distribution clearly shifts toward a higher temperautre with time. In particular, the mean state in the later period falls into the extreme end of preceding period, suggesting a siginicant increase in the likelihood of rare exteme event occurrence. Another interesting feature of the PDF shift is a really narrow distribution during 2014/15-2044/45 and a considerable broadening of the distribution with time in the future periods. This indicates small variability of and high consistence across the simulated Atlantic layer temperautres for the historical time. However, the variability and model uncertainties dramatically increase in the future projections. This dramatic increases might suggest that the Atlantic layer becomes unstable in a warming climate and the Arctic ocean circualtion is a grand challenge in model simulations. According to the PDFs

and following the same threshold of +1.5 standard deviation, the maximum probability of extremes increases from 6.7% to 18.3% during 2014/15-2044/45 and 75.4% during 2069/70-2098/99, respectively (**Table 1**). The temperautre anomaly of extreme warm events increases with the projected future gloable warming at 0.63ºC ºC^{-1} (**Fig. 5c, right**), suggesting an intensification of the extremes with the temperature anomaly reaching ~3.0ºC at the end of the 21st century.

[H2] Cryosphere

[H3] Sea ice extent

New decadal mean climate states have also consistently emerged for September sea ice concentration. September sea ice exhibits ToE spanning 1990-2010, with the earliest emergence occurring in the Eurasian Arctic (**Fig. 4d, left**). The much earlier occurrence of the sea ice ToE than SAT can be ascribed to enahnced albedo feedback along with the anthprogenically thinned ice. Like SST (**Fig. 4c**), the slightly later ToE north of Svalbard (~2015) occurs because of variability in ice transport through Fram Strait.

The existing transition into a new sea ice state increases the likelihood of future rapid sea ice loss events or extremes. One such change is an ice-free Arctic, considered an unprecedented extreme climate event completely out of the range of the historical records. In September, an ice-free Arctic could occur as early as the mid 21st century under all emissions scenarios[161,162,188–190]. Therefore, the PDF analysis only covers 1985-2014 and 2015-2044. The same as SAT and ocean temeprautres, the mean state of sea ice extent loss during the latter period falls into the extreme end of the former period (**Fig. 5d, left)**, indicating a considerable increase in the likelihood of rare extreme event occurrence. Speciffically, the maximum probability with the threshold of -1.5 standard deviation for the earlier period increases from 6.7% to 50.7% for the latter period (**Table 1**). The extreme sea ice extent loss events (<-1.5 standard deviation) intensify with the projected global mean summer SAT at a rate of -2.26 x 10^6 km^2 ºC^{-1} (**Fig. 5d, right)**, so that the extremely low sea ice extent from its historical maximum (~10.6 x 10^6 km^2 from multimodel mean) reaches -10.0 x 10^6 km^2 in the mid century, indicating an ice-free Arctic at this time. This time is consistent with the projections results of mean sea ice extent changes other studies[161,162,189,190]. Winter ice-free conditions are likely to appear by the late 21st century under the highest emissions scenarios[191,192].

[H3] Greenland Ice Sheet melt

Consistent with other variables across the Arctic climate system, annual GrIS melt rate anomaly also shows a climate state shift. The PDF distributions move toward a larger melt rarte with time (**Fig. 5e, left)**. One pronounced change is that the distribution during 2070-2099 is almost completely out of the range of the distribution during 1985-2014 and 2015-2044. This indicates that all rare extreme GrIS melt events before the mid century will likely become normal at the end of the century. Specifically, the maximum probability of rare melt events identified using the threshold of +1.5 standard deviation based on 1985-2014 increases from 6.7% to 57.2% during 2015-2044 and 100% during 2070-2099 (**Table 1**). All individual extreme melt events ((>+1.5 standard deviation) intensifies with the projected increase of global mean SAT (**Fig. 5e, right)**. The average melt rate anomaly of extreme events increases at a rate of 0.19 m year^{-1} ºC^{-1}, leading to a melt rate anomaly of 1.75 m year^{-1} at the end of the century.

[H1] Summary and future perspectives

Weather and climate extremes have systematically occurred across the Arctic climate system. Since ~2000, these events are occurring more frequently with increased amplitude. Indeed, the mean of Arctic SAT, precipitation, poleward ocean heat transport, ocean teamperature, sea ice extent and GrIS melt have all exhibited substantial shifts pre- and post-2000, with a corresponding change in the probability of rare

extremes. For instance, when using the +/-1.5 standard deviation based on the the period pre-2000 as the threshod to identify rare extreme events, the maximum probability of extreme variables across the Arctic climate system (including SAT, precipitation, Atlantic ocean heat transport, Atlantic layer temperature, upper ocean mixed layer temperautre, SST, sea ice extent loss from historical maximum, and GrIS melt extent) increase from ~6.7% pre-2000 to ~11.0% - 90.2% post-2000. This suggests that rare, low probability extreme events in some climate system components became high probability events post-2000. The occurrence of these Arctic extremes (and their step change ~2000) is related to pushing and triggering effects from multiscale and interactive processes. Long-term Arctic Amplification (and related thermodynamic effects) increase the vulnerability of the Arctic climate system to external forcing and internal perturbation, 'pushing' the system to approach a threshold or a tipping point[6,78,80,193]. Under the more vulnerable climate state, internal variability or externally-modulated internal variability can act as dynamical drivers to 'trigger' step changes of the climate to a new state with substantially increased frequency and intensity of extremes. Such pushing and triggering will continue into future with ongoing warming, and as such, Arctic extremes are set to further increase in frequency and amplitude. For instance, following the defined threshold of the +/-1.5 standard deviation from historical simulations, the maximum probability of projected extreme variables (including SAT, precipitation, Atlantic layer temperautre, upper ocean mixed layer temperautre, sea ice extent loss, and GrIS melt rate) increases from ~6.7% to ~17.3% - 57.2% in the mid century and to ~44.2% - 100.0% at the end of the century. Historically rare extreme events will likely be no longer rare.

Although progress has been made in understanding the characteristics and driving mechanisms of Arctic weather and climate extremes, research on this topic is in its infancy. Part of the challenge in synthesizing understanding of Arctic extremes is linked to different selection criteria used across research, for example thresholds of a certain magnitude or percentiles[194,195], or metrics of extreme intensity, duration or frequency. Therefore, an urgent priority should be to develop physically-based metrics that objectively and consistently define extremes[196], focusing on four groups: mean climate state shift; unprecedented events; rare low probability events; and unusually high impact events. Categorizing extremes into the four groups facilitate standardizing metrics for consistently identifying extreme events in each group considering the differences of temporal and spatial scales and driving mechanimes across the groups. For exmaple, mean climate state shift is a large scale event and can occur abruptly, which is well grounded on nonlinear dynamical systems[91]. Although several studies have postulated Arctic tipping elements and a possible shift of the Arctic climate to a new state[6,78,80,193,197], these studies have also raised questions about difficulties to objectively and accurately identify the tipping point and to define time scales of reversibility. These require innovative statistical or physical approaches to resolve based on improved understanding about nonlinear system. Similarly, other three groups of extremes also have distinct statistical and physical characteristics, respectively. With such consistent and physically-based metrics, systematic analayis of Arctic extremes can be achieved to identify common and essential climate features and driving mechanisms specific for each group alongside the typical case study approach utilized now.

The common challenge in furthering understanding across all four of these groups is the short and spatially sparse observational record. These limited observations offer limited case studies of extreme events and hinder establishing accurate and solid baseline climatology, which provides critical references for defining extreme events. Accordingly, it is crucial to develop a sustainable, high-resolution observational network as a basis for building a long-time database. Considering the harsh environment and limited accessibility in the Arctic, coordinated and systematic field observations (for example, carefully designed observational network through coordinating multi-country research vessels for capturing 3-dimensional picutre of the climate state from the deep ocean to the stratosphere) and new technologies (for example, improving satellite sensors to have high-resolution vertical profiles of atmospehric strucutre; improving data assimilation methods for effectively exploiting all possible observations from different sources) would be useful in this regard, with the latter specifically focused on fully coupled processes (for example, stratosphere impacts on cyclone genesis and development; deeper ocean heat release to sea ice and the atmosphere). Use of novel machine

learning and artificial intelligence methodologies also hold promise. These could be used to construct a database of Arctic extremes with increased spatio-temporal resolution, perhaps including reconstructed Arctic daily SATs and year-round sea ice thickness[84,198]. New reanalysis datasets, for example the Copernicus Arctic Regional Reanalysis at 2.5 km resolution[199,200] should also be assessed. While observations are integral for improved understanding, continually increasing high-resolution capability of Earth system models to realistically simulate multiscale Arctic processes is also necessary. Key priorities should be improving representation of stratospheric dynamics and high resolution ocean processes to realistically capture winter stratospheric polar vortex/summer lower stratospheric Arctic vortex, synergetic or competing effects between Arctic and lower latitude forcings, Atlantic and Pacific warm water inflow, ocean mixing and turbulent oceanic heat flux, AMOC and subpolar ocean gyres.

In addition to metric and data challenges, unanswered questions, uncertainties, debates and knowledge gaps persist. Many of these scientific unknowns relate to multiscale dynamic triggering processes in the context of long-term warming. For instance, although there is a clear association between Arctic extremes and SSWs[7,8], it is unknown whether the increasing trend of SSWs during 1980-2016 resulted from greenhouse gas forcing or natural variability[201]. Hence, it is unknown how these connections will evolve in the future, as evidenced by widely diverging SSW projections related to model errors[202]. An going effort to employ improved representation of the stratosphere in the Earth system models (for exmaple, the Whole Atmosphere Community Climate Model at NCAR[203]) to conduct large emsemble simulations and projections would be a way forward for reducing the uncertainties. In addition, the disagreement between the observed intensification of North Atlantic Ocean heat transport into the Arctic and the observed and projected weakening of AMOC raises challenging questions about what ocean processes drive the North Atlantic ocean heat transport into the Arctic[26,124,125,204]. The pulses of intense heat transport itself and resultant Atlantic layer temperautre anomalies can be extreme events, which might also precondition extreme sea ice loss and atmosphere and marine heatwave events. Therefore, a sustained, high resolution observations on vertical structures of ocean properties in the North Atlantic and Nordics Seas would facilitate solving the problem.

Problems also exist in detecting and understanding synoptic and mesoscale drivers and processes. Cyclones are a key synoptic drivers of Arctic extremes, yet their long-term changes with warming are uncertain owing to sensitivities to cyclone identification and tracking algorithms, analysis metrics characterizing cyclone activity, datasets, models and time periods[165,167,205–207]. Another emerging question is why anomalously intense and long-lasting cyclones have occurred more frequently during summer since the beginning of this century[13,140,142–144]. Although S-SAV/TPV intensifies and increases the persistence of summer cyclones[142–145], the generation of S-SAV and its coupling with cyclones are not well understood. Increase in model resolutions helps better capture finer-scale processes, but seems not able to completely solve the problems[208]. Optimization of cyclone tracking algorithms through intercomaprisons, development of intergrative cyclone activity metrics, temporally and spatially well covered vertical structure observations of the whole atmosphere, and improved stratosphere representation in models would help reduce uncertainties and enhance a robust understanding of cyclone changes.

Inconsistencies and debate have also arisen about cyclone impacts on sea ice and the ocean, as well as their feedbacks. Composite or regional aggregation analyses, for instance, raise debate about relative roles of cyclone-driven dynamic and thermodynamic effects on sea ice changes and the dependence of these effects on regions and seasons[36,37,209–211], because of highly seasonally and regionally-dependent radiation and ocean conditions in response to cyclones. Long-term changes in sea ice and ocean might also have altered large-scale driving mechanisms of cyclones to intensify cyclone activity[143,212,213], while cyclones might also feedback to further the changes in the sea ice and ocean[13,214], yet these feedback processes are not well understood. To solve these problems, comprehensive observations from the Atlantic and Pacific warm water layers of the ocean to sea ice and atmosphere during cyclone processes in different season and region are an imperative need. Improvement of model physics for realistically solving high-resolution coupling processes, including ocean mixing and turbulent fluxes across atmosphere, ocean, and sea ice interfaces, are critical.

The long-term warming has gradually changed characteristics of Arctic earth system and influence human activities. However, it is the weather and climate extremes that exert immediate and strong impacts, either

hazardous or beneficial, on daily life, societies, economics, and ecosystems[215,216,217]. These impacts can be amplified in the new Arctic climate state. Accordingly, there is a need to evaluate and quantify the social, economic and ecosystem impacts of extremes through engagement of social science community, policy-decision makers, and the the general public and intergaration of social impact module with the natural compoennts of Earth system models. Relatedly, prediction and predictability assessments for improving prediction skills, especially at subseasonal-to-seasonal scales, have arguably been the weakest element of the Arctic extremes research[218]. Thus, it would be a critical step forward to identify long-leading precursors and preconditioners through improved understanding of the multiscale, interactive "pushing and triggering" mechanisms by solving the problems discussed in this review.

References

1. Huang, J. *et al.* Recently amplified arctic warming has contributed to a continual global warming trend. *Nat. Clim. Change.* **7**, 875–879 (2017).
2. Lenssen, N. J. L. *et al.* Improvements in the GISTEMP uncertainty model. *J. Geophys. Res. Atmos.* **124**, 6307–6326 (2019).
3. Rohde, R. A. & Hausfather, Z. The berkeley earth Land/Ocean temperature record. *Earth Syst. Sci. Data* **12**, 3469–3479 (2020).
4. Morice, C. P. *et al.* An updated assessment of Near-Surface temperature change from 1850: the HadCRUT5 data set. *J. Geophys. Res. Atmos.* **126**, (2021).
5. Vose, R. S. *et al.* Implementing full spatial coverage in NOAA's global temperature analysis. *Geophys. Res. Lett.* **48**, (2021).
6. Zhang, X., Sorteberg, A., Zhang, J., Gerdes, R. & Comiso, J. C. Recent radical shifts of atmospheric circulations and rapid changes in Arctic climate system. *Geophys. Res. Lett.* **35**, (2008).
7. Moore, G. W. K. The december 2015 north pole warming event and the increasing occurrence of such events. *Sci. Rep.* **6**, (2016).
8. Overland, J. E. & Wang, M. Recent extreme Arctic temperatures are due to a split polar vortex. *J. Clim.* **29**, 5609–5616 (2016).
9. Kim, B.-M. *et al.* Major cause of unprecedented Arctic warming in january 2016: critical role of an atlantic windstorm. *Sci. Rep.* **7**, (2017).

10. Barkhordarian, A., Nielsen, D. M., Olonscheck, D. & Baehr, J. Arctic marine heatwaves forced by greenhouse gases and triggered by abrupt sea-ice melt. *Commun. Earth. Environ.* **5**, 57 (2024).
11. Parkinson, C. L. & Comiso, J. C. On the 2012 record low Arctic sea ice cover: Combined impact of preconditioning and an August storm. *Geophys. Res. Lett.* **40**, 1356–1361 (2013).
12. Graham, R. M. *et al.* Winter storms accelerate the demise of sea ice in the atlantic sector of the Arctic ocean. *Sci. Rep.* **9**, (2019).
13. Peng, L. *et al.* Role of Intense Arctic Storm in Accelerating Summer Sea Ice Melt: An In Situ Observational Study. *Geophys. Res. Lett.* **48**, e2021GL092714 (2021).
14. Zhang, X. *et al.* Enhanced poleward moisture transport and amplified northern high-latitude wetting trend. *Nat. Clim. Change.* **3**, 47–51 (2012).
15. Viceto, C. *et al.* Atmospheric rivers and associated precipitation patterns during the ACLOUD and PASCAL campaigns near svalbard (May-June 2017): case studies using observations, reanalyses, and a regional climate model. *Atmos. Chem. Phys.* **22**, 441–463 (2022).
16. Hansen, B. B. *et al.* Warmer and wetter winters: characteristics and implications of an extreme weather event in the high Arctic. *Environ. Res. Lett.* **9**, 114021 (2014).
17. Box, J. E. *et al.* Greenland ice sheet rainfall, heat and albedo feedback impacts from the Mid-August 2021 atmospheric river. *Geophys. Res. Lett.* **49**, (2022).
18. Peeters, B. *et al.* Spatiotemporal patterns of rain-on-snow and basal ice in high Arctic svalbard: detection of a climate-cryosphere regime shift. *Environ. Res. Lett.* **14**, 015002 (2019).
19. Cohen, J., Ye, H. & Jones, J. Trends and variability in rain-on-snow events. *Geophys. Res. Lett.* **42**, 7115–7122 (2015).
20. Bradley, J. A. *et al.* Svalbard winter warming is reaching melting point. *Nat. Commun.* **16**, 6409 (2025).
21. Stegall, S. T. & Zhang, J. Wind field climatology, changes, and extremes in the Chukchi-Beaufort seas and Alaska north slope during 1979-2009. *J. Clim.* **25**, 8075–8089 (2012).
22. Moore, G. W. K., Schweiger, A., Zhang, J. & Steele, M. What caused the remarkable february 2018 north greenland polynya? *Geophys. Res. Lett.* **45**, (2018).

23. Rheinlænder, J. *et al.* Driving mechanisms of an extreme winter sea-ice breakup event in the beaufort sea. *Geophys. Res. Lett.* (2022).
24. Mallett, R. D. C. *et al.* Record winter winds in 2020/21 drove exceptional Arctic sea ice transport. *Commun. Earth. Environ.* **2**, (2021).
25. Ingvaldsen, R. B. *et al.* Physical manifestations and ecological implications of Arctic Atlantification. *Nat. Rev. Earth Environ.* **2**, 874–889 (2021).
26. Tsubouchi, T. *et al.* Increased ocean heat transport into the nordic seas and Arctic ocean over the period 1993–2016. *Nat. Clim. Change.* **11**, 21–26 (2020).
27. A. Woodgate, R. & Peralta-Ferriz, C. Warming and freshening of the pacific inflow to the Arctic from 1990-2019 implying dramatic shoaling in pacific winter water ventilation of the Arctic water column. *Geophys. Res. Lett.* **48**, (2021).
28. Polyakov, I. V. *et al.* Greater role for atlantic inflows on sea-ice loss in the eurasian basin of the Arctic ocean. *Science.* **356**, 285–291 (2017).
29. Mattingly, K. S. *et al.* Strong summer atmospheric rivers trigger greenland ice sheet melt through spatially varying surface energy balance and cloud regimes. *J. Clim.* **33**, 6809–6832 (2020).
30. Mote, T. L. Greenland surface melt trends 1973-2007: evidence of a large increase in 2007. *Geophys. Res. Lett.* **34**, (2007).
31. Nghiem, S. V. *et al.* The extreme melt across the greenland ice sheet in 2012. *Geophys. Res. Lett.* **39**, (2012).
32. Screen, J. A. *et al.* Consistency and discrepancy in the atmospheric response to Arctic sea-ice loss across climate models. *Nat. Geosci.* **11**, 155–163 (2018).
33. Cohen, J. *et al.* Divergent consensuses on Arctic amplification influence on midlatitude severe winter weather. *Nat. Clim. Change.* **10**, 20–29 (2019).
34. Zhang, X. *et al.* Extreme Cold Events from East Asia to North America in Winter 2020/21: Comparisons, Causes, and Future Implications. *Adv. Atmos. Sci.* **39**, 553–565 (2022).

35. Semenov, A., Zhang, X., Rinke, A., Dorn, W. & Dethloff, K. Arctic intense summer storms and their impacts on sea Ice—A regional climate modeling study. *Atmosphere.* **10**, 218 (2019).
36. Clancy, R., Bitz, C. M., Blanchard-Wrigglesworth, E., McGraw, M. C. & Cavallo, S. M. A cyclone-centered perspective on the drivers of asymmetric patterns in the atmosphere and sea ice during Arctic cyclones. *J. Clim.* 1–47 (2022).
37. Aue, L., Vihma, T., Uotila, P. & Rinke, A. New insights into cyclone impacts on sea ice in the atlantic sector of the Arctic ocean in winter. *Geophys. Res. Lett.* **49**, (2022).
38. Malik, N. & Ozturk, U. Rare events in complex systems: understanding and prediction. *Chaos.* **30**, (2020).
39. Graham, R. M. *et al.* Increasing frequency and duration of Arctic winter warming events. *Geophys. Res. Lett.* **44**, 6974–6983 (2017).
40. Rigor, I. G., Colony, R. L. & Martin, S. Variations in surface air temperature observations in the arctic, 1979-97. *J. Clim.* **13**, 896–914 (2000).
41. Kobayashi, S. *et al.* The JRA-55 reanalysis: general specifications and basic characteristics. *J. Met. Soc. Jap. Ser. II.* **93**, 5–48 (2015).
42. Dee, D. P. *et al.* The ERA-Interim reanalysis: configuration and performance of the data assimilation system. *Q. J. R. Meteorol. Soc.* **137**, 553–597 (2011).
43. Boisvert, L. N., Petty, A. A. & Stroeve, J. C. The impact of the extreme winter 2015/16 Arctic cyclone on the Barents-Kara seas. *Mon. Wea. Rev.* **144**, 4279–4287 (2016).
44. Cullather, R. I. *et al.* Analysis of the warmest Arctic winter, 2015-2016. *Geophys. Res. Lett.* **43**, (2016).
45. Wentz, F. J. & Schabel, M. Precise climate monitoring using complementary satellite data sets. *Nature.* **403**, 414–416 (2000).
46. Held, I. M. & Soden, B. J. Robust responses of the hydrological cycle to global warming. *J. Clim.* **19**, 5686–5699 (2006).
47. Vihma, T. *et al.* The atmospheric role in the Arctic water cycle: a review on processes, past and future changes, and their impacts. *J. Geophys. Res. Biogeosci.* **121**, 586–620 (2016).
48. Serreze, M. C. & Barrett, A. P. Characteristics of the Beaufort Sea High. *J. Clim.* **24**, 159–182 (2011).

49. Zhang, X., Walsh, J. E., Zhang, J., Bhatt, U. S. & Ikeda, M. Climatology and Interannual Variability of Arctic Cyclone Activity: 1948–2002. *J. Clim.* **17**, 2300–2317 (2004).

50. Zhang, X. *et al.* Arctic cyclones have become more intense and longer-lived over the past seven decades. *Commun. Earth. Environ.* **4**, 348 (2023).

51. Gronas, S. & Skeie, P. A case study of strong winds at an Arctic front. *Tellus A.* **51**, 865–879 (1999).

52. Blanchard-Wrigglesworth, E., Webster, M., Boisvert, L., Parker, C. & Horvat, C. Record Arctic cyclone of january 2022: characteristics, impacts, and predictability. *J. Geophys. Res. Atmos.* **127**, (2022).

53. Årthun, M., Eldevik, T., Smedsrud, L. H., Skagseth, Ø. & Ingvaldsen, R. B. Quantifying the influence of atlantic heat on barents sea ice variability and retreat*. *J. Clim.* **25**, 4736–4743 (2012).

54. Steele, M. & Dickinson, S. The phenology of Arctic ocean surface warming. *J. Geophys. Res. Oceans.* **121**, 6847–6861 (2016).

55. Huang, B. *et al.* Prolonged marine heatwaves in the arctic: 1982-2020. *Geophys. Res. Lett.* **48**, (2021).

56. Timmermans, M.-L., Toole, J. & Krishfield, R. Warming of the interior Arctic ocean linked to sea ice losses at the basin margins. *Sci. Adv.* **4**, (2018).

57. Comiso, J. C., Parkinson, C. L., Gersten, R. & Stock, L. Accelerated decline in the Arctic sea ice cover. *Geophys. Res. Lett.* **35**, (2008).

58. Blunden, J. & Boyer, T. State of the climate in 2020. *Bull. Am. Meteorol. Soc.* **102**, S1–S475 (2021).

59. Årthun, M., Onarheim, I. H., Dörr, J. & Eldevik, T. The Seasonal and Regional Transition to an Ice-Free Arctic. *Geophys. Res. Lett.* **48**, e2020GL090825 (2021).

60. Rieke, O., Årthun, M. & Dörr, J. S. Rapid sea ice changes in the future Barents Sea. *The Cryosphere* **17**, 1445–1456 (2023).

61. Kwok, R. Arctic sea ice thickness, volume, and multiyear ice coverage: losses and coupled variability (1958-2018). *Environ. Res. Lett.* **13**, 105005 (2018).

62. Sumata, H., de Steur, L., Divine, D. V., Granskog, M. A. & Gerland, S. Regime shift in Arctic ocean sea ice thickness. *Nature.* **615**, 443–449 (2023).

63. Sumata, H., de Steur, L., Gerland, S., Divine, D. V. & Pavlova, O. Unprecedented decline of Arctic sea ice outflow in 2018. *Nat. Commun.* **13**, (2022).
64. Stroeve, J. & Notz, D. Changing state of Arctic sea ice across all seasons. *Environ. Res. Lett.* **13**, 103001 (2018).
65. Zheng, C. *et al.* Turbulent heat flux, downward longwave radiation, and Large-Scale atmospheric circulation associated with wintertime Barents-Kara sea extreme sea ice loss events. *J. Clim.* **35**, 3747–3765 (2022).
66. Ludwig, V. *et al.* The 2018 north greenland polynya observed by a newly introduced merged optical and passive microwave sea-ice concentration dataset. *Cryosphere.* **13**, 2051–2073 (2019).
67. Lee, Y. J. *et al.* Causes and evolution of winter polynyas north of greenland. *Cryosphere.* **17**, 233–253 (2023).
68. Shen, X. *et al.* Thinner sea ice contribution to the remarkable polynya formation north of greenland in August 2018. *Adv. Atmos. Sci.* **38**, 1474–1485 (2021).
69. Moore, G. W. K., Howell, S. E. L. & Brady, M. First observations of a transient polynya in the last ice area north of ellesmere island. *Geophys. Res. Lett.* **48**, (2021).
70. Parkinson, C. L. Arctic sea ice coverage from 43 years of satellite passive-microwave observations. *Front. Remote Sens.* **3**, (2022).
71. The IMBIE Team. Mass balance of the greenland ice sheet from 1992 to 2018. *Nature.* **579**, 233–239 (2019).
72. Hanna, E. *et al.* Increased runoff from melt from the greenland ice sheet: a response to global warming. *J. Clim.* **21**, 331–341 (2008).
73. Fettweis, X. *et al.* Brief communication 'important role of the mid-tropospheric atmospheric circulation in the recent surface melt increase over the greenland ice sheet'. *Cryosphere.* **7**, 241–248 (2013).
74. Tedesco, M. *et al.* Evidence and analysis of 2012 greenland records from spaceborne observations, a regional climate model and reanalysis data. *Cryosphere.* **7**, 615–630 (2013).

75. Hanna, E. *et al.* Atmospheric and oceanic climate forcing of the exceptional greenland ice sheet surface melt in summer 2012. *Int. J. Climatol.* **34**, 1022–1037 (2013).
76. Tedesco, M. & Fettweis, X. Unprecedented atmospheric conditions (1948-2019) drive the 2019 exceptional melting season over the greenland ice sheet. *Cryosphere.* **14**, 1209–1223 (2020).
77. Ing, R. N., Nienow, P. W., Sole, A. J., Tedstone, A. J. & Mankoff, K. D. Minimal Impact of Late-Season Melt Events on Greenland Ice Sheet Annual Motion. *Geophys. Res. Lett.* **51**, e2023GL106520 (2024).
78. Jeffries, M. O., Overland, J. E. & Perovich, D. K. The Arctic shifts to a new normal. *Phys. Today.* **66**, 35–40 (2013).
79. Drijfhout, S. *et al.* Catalogue of abrupt shifts in intergovernmental panel on climate change climate models. *Proc. Natl. Acad. Sci.* **112**, (2015).
80. Lenton, T. M. *et al.* Climate tipping points — too risky to bet against. *Nature.* **575**, 592–595 (2019).
81. Rocha, J. C., Peterson, G., Bodin, Ö. & Levin, S. Cascading regime shifts within and across scales. *Science.* **362**, 1379–1383 (2018).
82. Armstrong McKay, D. I. *et al.* Exceeding 1.5°c global warming could trigger multiple climate tipping points. *Science.* **377**, (2022).
83. Lenton, T. M. Early warning of climate tipping points. *Nat. Clim. Change.* **1**, 201–209 (2011).
84. Ma, Z. *et al.* Newly reconstructed Arctic surface air temperatures for 1979-2021 with deep learning method. *Sci. Data.* **10**, (2023).
85. Pithan, F. & Mauritsen, T. Arctic amplification dominated by temperature feedbacks in contemporary climate models. *Nat. Geosci.* **7**, 181–184 (2014).
86. Feldl, N., Po-Chedley, S., Singh, H. K. A., Hay, S. & Kushner, P. J. Sea ice and atmospheric circulation shape the high-latitude lapse rate feedback. *NPJ. Clim. Atmos. Sci.* **3**, (2020).
87. Boeke, R. C., Taylor, P. C. & Sejas, S. A. On the nature of the arctic's positive Lapse-Rate feedback. *Geophys. Res. Lett.* **48**, (2021).
88. Zhang, R. *et al.* Understanding the cold season Arctic surface warming trend in recent decades. *Geophys. Res. Lett.* **48**, (2021).

89. Taylor, P. C. *et al.* Process drivers, Inter-Model spread, and the path forward: a review of amplified Arctic warming. *Front. Earth Sci.* **9**, (2022).

90. Otosaka, I. N. *et al.* Mass balance of the Greenland and Antarctic ice sheets from 1992 to 2020. *Earth Syst. Sci. Data* **15**, 1597–1616 (2023).

91. Palmer, T. N. A nonlinear dynamical perspective on climate prediction. *J. Clim.* **12**, 575–591 (1999).

92. Hannachi, Abdel., Straus, D. M., Franzke, C. L. E., Corti, S. & Woollings, T. Low-frequency nonlinearity and regime behavior in the northern hemisphere extratropical atmosphere. *Rev. Geophys.* **55**, 199–234 (2017).

93. Thompson, D. W. J., Wallace, J. M. & Hegerl, G. C. Annular modes in the extratropical circulation. part II: trends. *J. Clim.* **13**, 1018–1036 (2000).

94. Hurrell, J. W., Kushnir, Y., Ottersen, G. & Visbeck, M. An overview of the North Atlantic Oscillation. in *Geophysical Monograph Series* (eds. Hurrell, J. W., Kushnir, Y., Ottersen, G. & Visbeck, M.) vol. 134 1–35 (American Geophysical Union, Washington, D. C., 2003).

95. Crasemann, B. *et al.* Can preferred atmospheric circulation patterns over the North-Atlantic-Eurasian region be associated with arctic sea ice loss? *Polar. Sci.* **14**, 9–20 (2017).

96. Jaiser, R. *et al.* Linkages between Arctic and Mid-Latitude weather and climate: unraveling the impact of changing sea ice and sea surface temperatures during winter. *Meteorol. Z.* **32**, 173–194 (2023).

97. Riebold, J. *et al.* On the linkage between future Arctic sea ice retreat, Euro-Atlantic circulation regimes and temperature extremes over europe. *Weather Clim. Dynam.* **4**, 663–682 (2023).

98. Rigor, I. G., Wallace, J. M. & Colony, R. L. Response of sea ice to the Arctic oscillation. *J. Clim.* **15**, 2648–2663 (2002).

99. Zhang, X., Ikeda, M. & Walsh, J. E. Arctic sea ice and freshwater changes driven by the atmospheric leading mode in a coupled sea Ice-Ocean model. *J. Clim.* **16**, 2159–2177 (2003).

100. Overland, J. E. & Wang, M. The Arctic climate paradox: the recent decrease of the Arctic oscillation. *Geophys. Res. Lett.* **32**, (2005).

101. Woollings, T., Hannachi, A., Hoskins, B. & Turner, A. A regime view of the north atlantic oscillation and its response to anthropogenic forcing. *J. Clim.* **23**, 1291–1307 (2010).

102. Woods, C., Caballero, R. & Svensson, G. Large-scale circulation associated with moisture intrusions into the Arctic during winter. *Geophys. Res. Lett.* **40**, 4717–4721 (2013).

103. Graversen, R. G., Mauritsen, T., Drijfhout, S., Tjernström, M. & Mårtensson, S. Warm winds from the pacific caused extensive Arctic sea-ice melt in summer 2007. *Clim. Dyn.* **36**, 2103–2112 (2010).

104. Moon, W., Kim, B.-M., Yang, G.-H. & Wettlaufer, J. S. Wavier jet streams driven by zonally asymmetric surface thermal forcing. *Proc. Natl. Acad. Sci.* **119**, (2022).

105. Overland, J. E. & Wang, M. Large-scale atmospheric circulation changes are associated with the recent loss of Arctic sea ice. *Tellus A.* **62**, 1 (2010).

106. Chen, H. W., Zhang, Q., Körnich, H. & Chen, D. A robust mode of climate variability in the Arctic: The Barents Oscillation. *Geophys. Res. Lett.* **40**, 2856–2861 (2013).

107. Clancy, R., Bitz, C. & Blanchard-Wrigglesworth, E. The influence of ENSO on Arctic sea ice in large ensembles and observations. *Journal of Climate* 1–50 (2021).

108. Ding, Q. *et al.* Fingerprints of internal drivers of Arctic sea ice loss in observations and model simulations. *Nat. Geosci.* **12**, 28–33 (2019).

109. Luo, B. *et al.* Origins of Barents-Kara sea-ice interannual variability modulated by the Atlantic pathway of El Niño–Southern Oscillation. *Nat. Commun.* **14**, 585 (2023).

110. Screen, J. A. & Francis, J. A. Contribution of sea-ice loss to Arctic amplification is regulated by Pacific Ocean decadal variability. *Nat. Clim. Change.* **6**, 856–860 (2016).

111. Kim, H., Yeh, S.-W., An, S.-I. & Song, S.-Y. Changes in the role of Pacific decadal oscillation on sea ice extent variability across the mid-1990s. *Sci. Rep.* **10**, 17564 (2020).

112. Chylek, P., Folland, C. K., Lesins, G., Dubey, M. K. & Wang, M. Arctic air temperature change amplification and the atlantic multidecadal oscillation. *Geophys. Res. Lett.* **36**, (2009).

113. Miles, M. W. *et al.* A signal of persistent Atlantic multidecadal variability in Arctic sea ice. *Geophys. Res. Lett.* **41**, 463–469 (2014).

114. Chen, X. & Dai, A. Quantifying Contributions of External Forcing and Internal Variability to Arctic Warming During 1900–2021. *Earth's Future* **12**, e2023EF003734 (2024).

115. Wang, Q., Shu, Q. & Wang, F. Recent emergence of Arctic atlantification dominated by climate warming. *Sci. Adv.* **10**, eadq5235 (2024).

116. Kim, B.-M. *et al.* Weakening of the stratospheric polar vortex by Arctic sea-ice loss. *Nat. Commun.* **5**, (2014).

117. Seviour, W. J. M. Weakening and shift of the Arctic stratospheric polar vortex: internal variability or forced response? *Geophys. Res. Lett.* **44**, 3365–3373 (2017).

118. Kretschmer, M. *et al.* More-persistent weak stratospheric polar vortex states linked to cold extremes. *Bull. Am. Meteorol. Soc.* **99**, 49–60 (2018).

119. King, A. D., Butler, A. H., Jucker, M., Earl, N. O. & Rudeva, I. Observed relationships between sudden stratospheric warmings and european climate extremes. *J. Geophys. Res. Atmos.* **124**, 13943–13961 (2019).

120. White, C. J. *et al.* Potential applications of subseasonal-to-seasonal (S2S) predictions. *Meteorol. Appl.* **24**, 315–325 (2017).

121. Domeisen, D. I. V. & Butler, A. H. Stratospheric drivers of extreme events at the earth's surface. *Commun. Earth. Environ.* **1**, (2020).

122. Årthun, M. *et al.* Skillful prediction of northern climate provided by the ocean. *Nat. Commun.* **8**, (2017).

123. Yeager, S. G., Karspeck, A. R. & Danabasoglu, G. Predicted slowdown in the rate of atlantic sea ice loss. *Geophys. Res. Lett.* **42**, (2015).

124. Bryden, H. L. *et al.* Reduction in ocean heat transport at 26°n since 2008 cools the eastern subpolar gyre of the north atlantic ocean. *J. Clim.* **33**, 1677–1689 (2020).

125. Weijer, W., Cheng, W., Garuba, O. A., Hu, A. & Nadiga, B. T. Cmip6 models predict significant 21st century decline of the atlantic meridional overturning circulation. *Geophys. Res. Lett.* **47**, (2020).

126. Dosser, H. V., Chanona, M., Waterman, S., Shibley, N. C. & Timmermans, M. -L. Changes in internal Wave-Driven mixing across the Arctic ocean: finescale estimates from an 18-year Pan-Arctic record. *Geophys. Res. Lett.* **48**, (2021).

127. Montiel, F., Squire, V. A., Doble, M., Thomson, J. & Wadhams, P. Attenuation and directional spreading of ocean waves during a storm event in the autumn beaufort sea marginal ice zone. *J. Geophys. Res. Oceans.* **123**, 5912–5932 (2018).

128. Jackson, J. M., Carmack, E. C., McLaughlin, F. A., Allen, S. E. & Ingram, R. G. Identification, characterization, and change of the near-surface temperature maximum in the canada basin, 1993-2008. *J. Geophys. Res. Oceans.* **115**, (2010).

129. Sledd, A., L'Ecuyer, T. S., Kay, J. E. & Steele, M. Clouds increasingly influence Arctic sea surface temperatures as CO2 rises. *Geophys. Res. Lett.* **50**, (2023).

130. Goosse, H. *et al.* Quantifying climate feedbacks in polar regions. *Nat. Commun.* **9**, 1919 (2018).

131. Zhang, J., Lindsay, R., Schweiger, A. & Rigor, I. Recent changes in the dynamic properties of declining Arctic sea ice: a model study. *Geophys. Res. Lett.* **39**, (2012).

132. Crews, L., Lee, C. M., Rainville, L. & Thomson, J. Direct observations of the role of lateral advection of sea ice meltwater in the onset of autumn freeze up. *J. Geophys. Res. Oceans.* **127**, (2022).

133. Sorteberg, A. & Walsh, J. E. Seasonal cyclone variability at 70°n and its impact on moisture transport into the Arctic. *Tellus A.* **60**, 570–586 (2008).

134. Jakobson, E. & Vihma, T. Atmospheric moisture budget in the Arctic based on the ERA-40 reanalysis. *Int. J. Climatol.* **30**, 2175–2194 (2010).

135. Dufour, A., Zolina, O. & Gulev, S. K. Atmospheric moisture transport to the arctic: assessment of reanalyses and analysis of transport components. *J. Clim.* **29**, 5061–5081 (2016).

136. Villamil-Otero, G. A., Zhang, J., He, J. & Zhang, X. Role of extratropical cyclones in the recently observed increase in poleward moisture transport into the Arctic Ocean. *Adv. Atmos. Sci.* **35**, 85–94 (2018).

137. Webster, M. A., Parker, C., Boisvert, L. & Kwok, R. The role of cyclone activity in snow accumulation on Arctic sea ice. *Nat. Commun.* **10**, (2019).

138. Duarte, P. *et al.* Warm atlantic water explains observed sea ice melt rates north of svalbard. *J. Geophys. Res. Oceans.* **125**, (2020).

139. Zhang, J., Lindsay, R., Schweiger, A. & Steele, M. The impact of an intense summer cyclone on 2012 Arctic sea ice retreat. *Geophys. Res. Lett.* **40**, 720–726 (2013).

140. Simmonds, I. & Rudeva, I. The great Arctic cyclone of August 2012. *Geophys. Res. Lett.* **39**, 2012GL054259 (2012).

141. Zhang, J., Zhang, X., Walsh, J. E., Roesler, E. & Hillman, B. Concurrence of blowing snow and polynya enhances arctic surface-atmosphere interaction: a modeling study with an extreme wind event in 2018. *Environ. Res. Climate.* **2**, 011004 (2023).

142. Aizawa, T. & Tanaka, H. L. Axisymmetric structure of the long lasting summer Arctic cyclones. *Polar. Sci.* **10**, 192–198 (2016).

143. Tao, W., Zhang, J. & Zhang, X. The role of stratosphere vortex downward intrusion in a long-lasting late-summer Arctic storm. *Q. J. R. Meteorol. Soc.* **143**, 1953–1966 (2017).

144. Tao, W., Zhang, J., Fu, Y. & Zhang, X. Driving Roles of Tropospheric and Stratospheric Thermal Anomalies in Intensification and Persistence of the Arctic Superstorm in 2012. *Geophys. Res. Lett.* **44**, (2017).

145. Vessey, A. F., Hodges, K. I., Shaffrey, L. C. & Day, J. J. The composite development and structure of intense synoptic-scale Arctic cyclones. *Weather Clim. Dynam.* **3**, 1097–1112 (2022).

146. Bray, M. T. & Cavallo, S. M. Characteristics of long-track tropopause polar vortices. *Weather Clim. Dynam.* **3**, 251–278 (2022).

147. Hanna, E. *et al.* Greenland surface air temperature changes from 1981 to 2019 and implications for ice-sheet melt and mass-balance change. *Int. J. Climatol.* **41**, (2020).

148. Binder, H. *et al.* Exceptional air mass transport and dynamical drivers of an extreme wintertime Arctic warm event. *Geophys. Res. Lett.* **44**, (2017).

149. Wang, Z., Walsh, J., Szymborski, S. & Peng, M. Rapid Arctic sea ice loss on the synoptic time scale and related atmospheric circulation anomalies. *J. Clim.* **33**, 1597–1617 (2020).

150. *An Introduction to Atmospheric Radiation*. (Academic Press, Amsterdam Boston, 2002).

151. Mattingly, K. S., Mote, T. L. & Fettweis, X. Atmospheric River Impacts on Greenland Ice Sheet Surface Mass Balance. *JGR Atmospheres* **123**, 8538–8560 (2018).

152. Li, L. *et al.* Impact of atmospheric rivers on Arctic sea ice variations. *The Cryosphere* **18**, 121–137 (2024).

153. Ma, W. *et al.* Wintertime extreme warming events in the high Arctic: characteristics, drivers, trends, and the role of atmospheric rivers. *Atmos. Chem. Phys.* **24**, 4451–4472 (2024).

154. Zhang, P. *et al.* More frequent atmospheric rivers slow the seasonal recovery of Arctic sea ice. *Nat. Clim. Change.* **13**, 266–273 (2023).

155. Bromwich, D. H. Polar Lows: Mesoscale Weather Systems in the Polar Regions. *Eos. Trans. AGU.* **85**, 121–121 (2004).

156. Landgren, O. A., Seierstad, I. A. & Iversen, T. Projected future changes in Marine Cold-Air Outbreaks associated with Polar Lows in the Northern North-Atlantic Ocean. *Clim. Dyn.* **53**, 2573–2585 (2019).

157. Gong, X. *et al.* Arctic warming by abundant fine sea salt aerosols from blowing snow. *Nature. Geosci.* **16**, 768–774 (2023).

158. Cai, Z. *et al.* Arctic warming revealed by multiple CMIP6 models: evaluation of historical simulations and quantification of future projection uncertainties. *J. Clim.* **34**, 4871–4892 (2021).

159. Hahn, L. C., Armour, K. C., Zelinka, M. D., Bitz, C. M. & Donohoe, A. Contributions to polar amplification in CMIP5 and CMIP6 models. *Front. Earth Sci.* **9**, (2021).

160. Shu, Q. *et al.* Arctic ocean amplification in a warming climate in CMIP6 models. *Sci. Adv.* **8**, (2022).

161. Notz, D. & Community, S. Arctic sea ice in CMIP6. *Geophys. Res. Lett.* **47**, (2020).

162. Zhang, X. Sensitivity of arctic summer sea ice coverage to global warming forcing: towards reducing uncertainty in arctic climate change projections. *Tellus A: Dyn. Meteorol. Oceanogr.* **62**, 220–227 (2010).

163. Landrum, L. & Holland, M. M. Extremes become routine in an emerging new Arctic. *Nat. Clim. Change.* **10**, 1108–1115 (2020).

164. Lee, J.-Y. & Marotzke, J. Future Global Climate: Scenario-based Projections and Near-term Information. in *Climate Change 2021 – The Physical Science Basis* 553–672 (Cambridge University Press, 2023).

165. Orsolini, Y. J. & Sorteberg, A. Projected changes in eurasian and Arctic summer cyclones under global warming in the bergen climate model. *Atmos. Ocean. Sci. Lett.* **2**, 62–67 (2009).

166. Akperov, M. *et al.* Future projections of cyclone activity in the Arctic for the 21st century from regional climate models (Arctic-CORDEX). *Glob. Planet. Change.* **182**, 103005 (2019).

167. Day, J. J., Holland, M. M. & Hodges, K. I. Seasonal differences in the response of Arctic cyclones to climate change in CESM1. *Clim. Dyn.* **50**, 3885–3903 (2017).

168. Nishii, K., Nakamura, H. & Orsolini, Y. J. Arctic summer storm track in CMIP3/5 climate models. *Clim. Dyn.* **44**, 1311–1327 (2014).

169. Parker, C. L., Mooney, P. A., Webster, M. A. & Boisvert, L. N. The influence of recent and future climate change on spring Arctic cyclones. *Nat. Commun.* **13**, (2022).

170. Zhang, L., Zhao, Y., Cheng, T. F. & Lu, M. Future Changes in Global Atmospheric Rivers Projected by CMIP6 Models. *J. Geophys. Res. Atmos.* **129**, e2023JD039359 (2024).

171. Zahn, M. & von Storch, H. Decreased frequency of north atlantic polar lows associated with future climate warming. *Nature.* **467**, 309–312 (2010).

172. Romero, R. & Emanuel, K. Climate change and Hurricane-Like extratropical cyclones: projections for north atlantic polar lows and medicanes based on CMIP5 models. *J. Clim.* **30**, 279–299 (2017).

173. Landgren, O. A., Batrak, Y., Haugen, J. E., Støylen, E. & Iversen, T. Polar low variability and future projections for the nordic and barents seas. *Q. J. R. Meteorol. Soc.* **145**, 3116–3128 (2019).

174. Bresson, H., Hodges, K. I., Shaffrey, L. C., Zappa, G. & Schiemann, R. The response of northern hemisphere polar lows to climate change in a 25 km High-Resolution global climate model. *J. Geophys. Res. Atmos.* **127**, (2022).

175. Kay, J. E. *et al.* The community earth system model (CESM) large ensemble project: a community resource for studying climate change in the presence of internal climate variability. *Bull. Am. Meteorol. Soc.* **96**, 1333–1349 (2015).

176. Eyring, V. *et al.* Overview of the Coupled Model Intercomparison Project Phase 6 (CMIP6) experimental design and organization. *Geosci. Model Dev.* **9**, 1937–1958 (2016).

177. Park, J.-Y. *et al.* Future sea-level projections with a coupled atmosphere-ocean-ice-sheet model. *Nat. Commun.* **14**, 636 (2023).

178. Li, C. *et al.* Changes in annual extremes of daily temperature and precipitation in CMIP6 models. *J. Clim.* **34**, 3441–3460 (2021).

179. Bintanja, R. & Andry, O. Towards a rain-dominated Arctic. *Nat. Clim. Change.* **7**, 263–267 (2017).

180. McCrystall, M. R., Stroeve, J., Serreze, M., Forbes, B. C. & Screen, J. A. New climate models reveal faster and larger increases in Arctic precipitation than previously projected. *Nat. Commun.* **12**, (2021).

181. Bintanja, R. & Selten, F. M. Future increases in Arctic precipitation linked to local evaporation and sea-ice retreat. *Nature.* **509**, 479–482 (2014).

182. Kattsov, V. M. *et al.* Simulation and projection of Arctic freshwater budget components by the IPCC AR4 global climate models. *J. Hydrometeorol.* **8**, 571–589 (2007).

183. Mioduszewski, J., Vavrus, S. & Wang, M. Diminishing Arctic sea ice promotes stronger surface winds. *J. Clim.* **31**, 8101–8119 (2018).

184. Ruosteenoja, K., Vihma, T. & Venäläinen, A. Projected changes in european and north atlantic seasonal wind climate derived from CMIP5 simulations. *J. Clim.* **32**, 6467–6490 (2019).

185. Meylan, M. H., Perrie, W., Toulany, B., Hu, Y. & Casey, M. P. On the Three-Dimensional scattering of waves by flexible marginal ice floes. *J. Geophys. Res. Oceans.* **125**, (2020).

186. Perrie, W., Meylan, M. H., Toulany, B. & Casey, M. P. Modelling wave-ice interactions in three dimensions in the marginal ice zone. *Phil. Trans. R. Soc. A.* **380**, (2022).

187. He, Y. *et al.* Arctic Amplification of marine heatwaves under global warming. *Nat. Commun.* **15**, 8265 (2024).

188. Wang, M. & Overland, J. E. A sea ice free summer Arctic within 30 years? *Geophys. Res. Lett.* **36**, (2009).

189. Kim, Y.-H., Min, S.-K., Gillett, N. P., Notz, D. & Malinina, E. Observationally-constrained projections of an ice-free Arctic even under a low emission scenario. *Nat. Commun.* **14**, (2023).

190. Shen, Z., Zhou, W., Li, J. & Chan, J. C. L. A frequent ice-free Arctic is likely to occur before the mid-21st century. *NPJ. Clim. Atmos. Sci.* **6**, (2023).

191. Hankel, C. & Tziperman, E. The role of atmospheric feedbacks in abrupt winter Arctic sea ice loss in future warming scenarios. *J. Clim.* **34**, 4435–4447 (2021).

192. Keen, A. *et al.* An inter-comparison of the mass budget of the Arctic sea ice in CMIP6 models. *Cryosphere.* **15**, 951–982 (2021).

193. Lenton, T. M. *et al.* Tipping elements in the earth's climate system. *Proc. Natl. Acad. Sci.* **105**, 1786–1793 (2008).

194. Easterling, D. R. *et al.* Observed variability and trends in extreme climate events: a brief review*. *Bull. Am. Meteorol. Soc.* **81**, 417–425 (2000).

195. Seneviratne, S. I. *et al.* Changes in Climate Extremes and their Impacts on the Natural Physical Environment. in *Managing the Risks of Extreme Events and Disasters to Advance Climate Change Adaptation* (eds. Field, C. B., Barros, V., Stocker, T. F. & Dahe, Q.) 109–230 (Cambridge University Press, 2012).

196. Röthlisberger, M. *et al.* A new framework for identifying and investigating seasonal climate extremes. *J. Clim.* **34**, 7761–7782 (2021).

197. Bathiany, S., Hidding, J. & Scheffer, M. Edge detection reveals abrupt and extreme climate events. *J. Clim.* **33**, 6399–6421 (2020).

198. Landy, J. C. *et al.* A year-round satellite sea-ice thickness record from CryoSat-2. *Nature.* **609**, 517–522 (2022).

199. Køltzow, M., Schyberg, H., Støylen, E. & Yang, X. Value of the copernicus Arctic regional reanalysis (CARRA) in representing near-surface temperature and wind speed in the north-east european Arctic. *Polar. Res.* **41**, (2022).

200. Moore, G. W. K. & Imrit, A. A. Impact of resolution on the representation of the mean and extreme winds along nares strait. *J. Geophys. Res. Atmos.* **127**, (2022).

201. Dimdore-Miles, O., Gray, L. & Osprey, S. Origins of multi-decadal variability in sudden stratospheric warmings. *Weather Clim. Dynam.* **2**, 205–231 (2021).

202. Karpechko, A. Yu. *et al.* Northern hemisphere Stratosphere-Troposphere circulation change in CMIP6 models: 1. Inter-Model spread and scenario sensitivity. *J. Geophys. Res. Atmos.* **127**, (2022).

203. Gettelman, A. *et al.* The Whole Atmosphere Community Climate Model Version 6 (WACCM6). *JGR Atmospheres* **124**, 12380–12403 (2019).

204. Oldenburg, D., Armour, K. C., Thompson, L. & Bitz, C. M. Distinct mechanisms of ocean heat transport into the Arctic under internal variability and climate change. *Geophys. Res. Lett.* **45**, 7692–7700 (2018).

205. Sepp, M. & Jaagus, J. Changes in the activity and tracks of Arctic cyclones. *Clim. Change.* **105**, 577–595 (2010).

206. Valkonen, E., Cassano, J. & Cassano, E. Arctic cyclones and their interactions with the declining sea ice: a recent climatology. *J. Geophys. Res. Atmos.* **126**, (2021).

207. Vavrus, S. J. Extreme Arctic cyclones in CMIP5 historical simulations. *Geophys. Res. Lett.* **40**, 6208–6212 (2013).

208. Huo, Y. *et al.* E3SM-Arctic: Regionally Refined Coupled Model for Advanced Understanding of Arctic Systems Interactions. *J Adv Model Earth Syst* **17**, e2024MS004726 (2025).

209. Schreiber, E. A. P. & Serreze, M. C. Impacts of synoptic-scale cyclones on Arctic sea-ice concentration: a systematic analysis. *Ann. Glaciol.* **61**, 139–153 (2020).

210. Finocchio, P. M., Doyle, J. D. & Stern, D. P. Accelerated sea ice loss from late summer cyclones in the new Arctic. *J. Clim.* **35**, 7751–7769 (2022).

211. Aue, L. *et al.* Impact of three intense winter cyclones on the sea ice cover in the barents sea: a case study with a coupled regional climate model. *Front. Earth Sci.* **11**, (2023).

212. Day, J. J. & Hodges, K. I. Growing Land-Sea temperature contrast and the intensification of Arctic cyclones. *Geophys. Res. Lett.* **45**, 3673–3681 (2018).

213. Crawford, A. D., Lukovich, J. V., McCrystall, M. R., Stroeve, J. C. & Barber, D. G. Reduced sea ice enhances intensification of winter storms over the Arctic ocean. *J. Clim.* **35**, 3353–3370 (2022).

214. Heukamp, F. O., Kanzow, T., Wang, Q., Wekerle, C. & Gerdes, R. Impact of cyclonic wind anomalies caused by massive winter sea ice retreat in the barents sea on atlantic water transport toward the arctic: a model study. *J. Geophys. Res. Oceans.* **128**, (2023).

215. Walsh, J. E. *et al.* Extreme weather and climate events in northern areas: a review. *Earth Sci. Rev.* **209**, 103324 (2020).

216. Overland, J. E. Rare events in the Arctic. *Clim. Change.* **168**, (2021).

217. Mudryk, L. R. *et al.* Impact of 1, 2 and 4 °c of global warming on ship navigation in the canadian Arctic. *Nat. Clim. Change.* **11**, 673–679 (2021).

218. Biernat, K. A., Keyser, D. & Bosart, L. F. A climatological comparison of the Arctic environment and Arctic cyclones between periods of low and high forecast skill of the Synoptic-Scale flow. *Mon. Wea. Rev.* **151**, 1957–1978 (2023).

219. Hersbach, H. *et al.* The ERA5 global reanalysis. *Q. J. R. Meteorol. Soc.* **146**, 1999–2049 (2020).

220. Cheng, L. *et al.* IAPv4 ocean temperature and ocean heat content gridded dataset. *Earth Syst. Sci. Data* **16**, 3517–3546 (2024).

221. Mote, T. L. & Anderson, M. R. Variations in snowpack melt on the greenland ice sheet based on passive-microwave measurements. *J. Glaciol.* **41**, 51–60 (1995).

222. Siegert, M. J. *et al.* Antarctic extreme events. *Front. Environ. Sci.* **11**, (2023).

223. Scambos, T. A. *et al.* Ultralow surface temperatures in east antarctica from satellite thermal infrared mapping: the coldest places on earth. *Geophys. Res. Lett.* **45**, 6124–6133 (2018).

224. Xu, M. *et al.* Dominant role of vertical air flows in the unprecedented warming on the antarctic peninsula in february 2020. *Commun. Earth. Environ.* **2**, (2021).

225. Chetty, T. R. K. & Kehelpannala, K. V. W. East antarctica. in *Atlas of Deformed and Metamorphosed Rocks from Proterozoic Orogens* 315–372 (Elsevier, 2022).

226. Blanchard-Wrigglesworth, E., Cox, T., Espinosa, Z. I. & Donohoe, A. The largest ever recorded Heatwave—Characteristics and attribution of the antarctic heatwave of march 2022. *Geophys. Res. Lett.* **50**, (2023).

227. Terpstra, A., Gorodetskaya, I. V. & Sodemann, H. Linking Sub-Tropical evaporation and extreme precipitation over east antarctica: an atmospheric river case study. *J. Geophys. Res. Atmos.* **126**, (2021).

228. Yu, L. *et al.* Features of extreme precipitation at progress station, antarctica. *J. Clim.* **31**, 9087–9105 (2018).

229. Meehl, G. A. *et al.* Sustained ocean changes contributed to sudden antarctic sea ice retreat in late 2016. *Nat. Commun.* **10**, (2019).

230. Campbell, E. C. *et al.* Antarctic offshore polynyas linked to southern hemisphere climate anomalies. *Nature.* **570**, 319–325 (2019).

231. Turner, J. *et al.* Record low antarctic sea ice cover in february 2022. *Geophys. Res. Lett.* **49**, (2022).

232. Rott, H., Skvarca, P. & Nagler, T. Rapid collapse of northern larsen ice shelf, antarctica. *Science.* **271**, 788–792 (1996).

233. Rack, W. & Rott, H. Pattern of retreat and disintegration of the larsen b ice shelf, antarctic peninsula. *Ann. Glaciol.* **39**, 505–510 (2004).

234. Scambos, T. *et al.* Ice shelf disintegration by plate bending and hydro-fracture: satellite observations and model results of the 2008 wilkins ice shelf break-ups. *Earth Planet. Sci. Lett.* **280**, 51–60 (2009).

235. Rignot, E. *et al.* Accelerated ice discharge from the antarctic peninsula following the collapse of larsen b ice shelf. *Geophys. Res. Lett.* **31**, (2004).

Acknowledgements
This article is an outcome of the workshop "Arctic Climate and Weather Extremes: Detection, Attribution, and Future Projection", which was hosted by the Aspen Global Change Institute and supported by NASA's Earth Science Division Award #80NSSC20K1156, NOAA's Climate Program Office Award #NA22OAR4310117, NSF's programs for Arctic System Science (ARCSS) and Prediction of and Resilience against Extremes Events (PREEVENTS) Award #1934420, and International Arctic Science Committee (IASC). We also acknowledge the support of the U.S. Department of Energy (DOE) grant #DE-SC0024872 (X.Z. and H.T.), the computing resources with the projects m3638 and m4622 awarded by the DOE's National Energy Research Scientific Computing Center (NERSC) (X.Z., H.T., and J.Z.), the U.S. NOAA CISESS Agreement NA19NES4320002 (X.Z.), the PolarRES project #101003590 under the European Union's Horizon 2020 research and innovation programme (T.V., A.R., C.Ä., B.C., D.H.), the Natural Sciences and Engineering Research Council of Canada (G.W.K.M.), the NSF-NCAR sponsored by the U.S. NSF under the Cooperative Agreement 1852977 (A.D., L.L.), the National Key R&D Program of Change grant #2022YFE0106700 and the Norwegian Research Council grant #328957 (J.H., Y.L.), the National Nature Science Foundation of China grant #42430609 (C.L.), the the Deutsche Forschungsgemeinschaft project #268020496 TRR 172 within the Transregional Collaborative Research Center "ArctiC Amplification: Climate Relevant Atmospheric and SurfaCe Processes, and Feedback Mechanisms (AC)3" (D.H, A.R.), the German Federal Ministry for Research, Technology and Space project "TurbO-Arctic" (01LK2317A) of the "WarmWorld Smarter" Program (D.H.), the U.S. NOAA GOMO Arctic Research Program (J.O), the U.S. NASA grants #80NSSC20K0768 and #80NSSC21K0832, the U.S. NSF grant #OPP2138316, and the U.S. ONR grant N00014-21-1-2868 (M.S.), and the U.S. DOE RGMA program area as contribution to the HiLAT-RASM project (H.W., W.W.). W.T. was supported while serving at the the U.S. NSF; the findings and conclusions expressed herein do not necessarily reflect the views of the NSF or the U.S. Government.

Supplementary information [Au: DOI will be updated before publication. Please do not change]
Supplementary information is available for this paper at https://doi.org/10.1038/s415XX-XXX-XXXX-X

Publisher's note [Au: Needed because you have maps. Please do not delete or change]
Springer Nature remains neutral with regard to jurisdictional claims in published maps and institutional affiliations.

Competing interests
The authors declare no competing interests.

Author contributions
X.Z., T.V., A.R., and G.W.K.M. conceived the project and chaired a workshop on the topic. X.Z. constructed the manuscript content and structure based on discussions with coauthors. X.Z. led writing of the manuscript, researching data, and designing figures with incorporating suggestions and contributions from T.V., A.R., G.W.K.M, and all other coauthors. H.T., C.Ä, A.D., L.L., J.H., C.L., and J.Z. contributed to researching data and preparing figures. T.V. led writing of Text Box 1. L.B., B.C., A.D., J.O., K.S., M.S., and T.V. coordinated coauthors' contributions to various subsections of the initial version of the draft. All coauthors contributed to the discussion of content, writing, and review/editing of the manuscript and its revision.

Display items [Au: should be in the order Tables, figures, boxes]

Table 1. Maximum probability of extreme event occurrence using +/-1.5 standard deviation as the threshold for reference time periods in observations and model simulations and projections.

Figure 1. **Weather and climate extremes in the Arctic.** Select examples of extreme events in the Arctic climate system, including their drivers and impacts. Increased extreme events have been observed across the Arctic region in the atmosphere, ocean and cryosphere since ~2000, with impacts that extend across physical, ecological and social systems.

Figure 2. **Observed changes in Arctic extreme events**. **a,** The probability density function (PDF) distributions of winter (December - February) daily surface air temperature[219] (SAT) over the North Atlantic Arctic (75°N - 90°N, 0 - 90°E) in 1979/80 - 1999/2000 and 2000/01 - 2023/24 (left). The corresponding timeseries of winter SAT (right), including specific extreme events (labelled circles) and the linear trend (dashed line), as quantified in the box. Lighter and darker colors highlight the periods before and after the turn of the 21st century, respectively. The three layers of shading represent ±0.5, ±1.0 and ±1.5 standard deviations. **b,** as in a but for winter precipitation[219] in the North Atlantic Arctic (75°N - 90°N, 0 - 90°E). **c,** As in panel a, but for winter (October - March) poleward North Atlantic oceanic heat transport[26] into the Arctic Ocean and Nordic Seas, with PDFs comparing 1993/94 - 1999/2000 and 2000/01 - 2016/17. **d,** as in panel a but for winter (October - March) Atlantic water layer temperature[220] within the central Arctic, with PDFs comparing 1979/80 - 1999/2000 and 2000/21 - 2022/23. Atlantic water layer temperature is calculated as the thickness-weighted vertical average between 200 - 600 m) north of 70°N. **e,** As in panel a, but for September sea ice extent relative to its maximum[64], with the PDFs comparing 1979 - 1999 and 2000 - 2023. Sea ice extent relative to its maximum is chosen to indicate maximum sea ice extent loss, with the maximum value is identified over 1979 - 1999. **f,** As in panel a, but for summer maximum Greenland Ice Sheet melt extent[221], with the PDFs comparing 1979 - 1999 and 2000 - 2023. An increase in the frequency of Arctic weather and climate extremes exceeding +1.0 σ of their historical variability have coherently occurred across the Arctic climate system.

Figure 3. **The 'pushing and triggering' mechanisms. a**, Schematic representation of the mechanisms driving extreme Arctic events in the present day, including the mean climate state shift ~2000. Pushing mechanisms describe anthropogenic warming effects destabilizing the Arctic climate system to become more vulnerable (bold face text), and triggering mechanisms indicate the role of multi-scale atmosphere, ocean, and sea ice dynamics in initating and driving extreme events (normal text); see also Supplementary Figure 12. **b,** as in panel a but for the projected future. Anthropogenic warming and nonlinear atmosphere, ocean and sea ice dynamics have 'pushing and triggering' roles that increase the frequency of Arctic weather and climate extremes.

Figure 4. **Projected Time of Emergence in the Arctic**. **a,** Time of Emergence (ToE) for February surface air temperature (left), and at a selected point north of Svalbard (right; black dot on the left map). ToE is defined as the year when the model ensemble mean (blue solid line) crosses the $\pm$2.0 standard deviation (red solid line) from the baseline climate state in 1920-1929. Data are from the Community Earth System Model version 1 Large Ensemble (CESM-LE)[175], under RCP8.5 scenario. **b,** As in panel **a**, but for the length of annual snow season (left), and the first day of annual rain season north of Svalbard (right). **c**, As in panel **a**, but for August sea surface temperature. **d**, As in panel **a**, but for September sea ice concentration. Extreme shifts have occurred, or can soon expect to occur, in the state of the Arctic climate system largely beyond what the baseline climate variability explains.

Figure 5. Projected future changes in Arctic extremes. a, Simulated probability density function (PDF) distributions of winter (December - February) daily surface air temperature (SAT) anomaly over the North Atlantic Arctic (75°N - 90°N; 0 - 90°E) in 1984/85 - 2013/14, 2014/15 - 2044/45 and 2069/70 - 2098/99 (left). Changes in North Atlantic Arctic extreme warm events (SAT anomaly exceeding a threshold of +2.0 standard deviation) with global mean SAT increase. Data are from CMIP6 multi-model projections[176]

(Supplementary Table 2), with only one ensemble member chosen from each model to reduce interconnections between model projections. **b**, As in panel **a**, but for winter precipitation over the North Atlantic Arctic (left), and changes in extreme precipitation events (precipitation anomaly exceeding a threshold of +2.0 standard deviation) with the global mean SAT increase (right). **c,** As in panel a, but for winter (October – March) Atlantic water layer ocean temperature in the central Arctic (70°N – 90°N; left), and changes in winter Atlantic water layer extreme warm events (ocean temperature anomaly exceeding a threshold of +1.5 standard deviation) with global mean SAT increase (right). Atlantic water layer temperature is calculated as thickness-weighted anomalies between 200 – 600 m. **d,** As in panel a, but for September monthly sea ice extent relative to the 1985-2014 maximum (left), and changes in extreme September sea ice extent loss (anomalies exceeding a threshold of +1.5 standard deviation) with global mean SAT increase (right). Given a projected ice-free Arctic Ocean after the mid 21st century, the PDF analysis does not cover the time period from 2070 – 2099. **e**, As in panel a, but for annual Greenland Ice Sheet surface melt rate anomaly[177], with PDFs calculated over 1985 – 2014, 2015 – 2045 and 2070 – 2099 (left); and changes in extreme Greenland Ice Sheet surface melt rate events[177] (surface melt rate anomaly exceeding a threshold of +1.5 standard deviation) with global mean SAT increase (right). The extreme events are identified using a moving 20-year time window with an interval of 5-year between two windows. Arctic weather and climate extremes are projected to occur more frequently and with greater magnitude in the future.

Box 1 | **Antarctic weather and climate extremes**

At the circumpolar scale, the Antarctic climate system has experience less dramatic changes compared to the Arctic. However, regional weather and climate extremes have been prominent in the Antarctic[222].

The record-lowest 2-m air temperature observed in the Antarctic dates back to 21 July 1983, when -89.2°C was observed at the Vostok station in East Antarctica. Due to the sparsity of observations, it does not necessarily represent the coldest weather event in Antarctica. Satellite thermal infrared mapping has revealed snow surface temperatures of approximately -98°C in several small topographic basins in high-elevation East Antarctica during winters of 2004–2016[223]. These were estimated to correspond to 2-m air temperatures of approximately -94°C. The warmest 2-m air temperature ever observed in the Antarctic continent, 18.3°C, occurred at the Argentinian Esperanza station on the northern tip of the Antarctic Peninsula on 6 February 2020. The event was associated with anticyclonic circulation bringing a warm, moist air mass from the Pacific Ocean to the Antarctic Peninsula, and a strong Foehn downslope of the Peninsula mountains made the downslope flow record warm[224]. An extreme heatwave occurred over East Antarctica on 15-19 March 2022. Widespread warm anomalies reached 30-45°C, driven by an extremely intense atmospheric river[225,226]. It transported heat and moisture from the sea south of Australia far to the high plateau of East Antarctica. In addition to extreme temperatures, atmospheric rivers are often responsible for extreme precipitation events in coastal regions of Antarctica[227]. Such events have become more common and more intense[228].

A prominent climate extreme was the sudden decline of Antarctic sea-ice extent in late 2016, after three decades of increase. The decline was preconditioned by warming of surface waters and thinning of sea ice in the Southern Ocean, and occurred due to extreme atmosphere-ocean anomalies in the eastern tropical Indian and far-western Pacific Oceans[229]. These anomalies triggered atmospheric planetary wave trains that propagated to the Antarctic, generated wind anomalies, changed the sea-ice patterns, and reversed the hemispheric sea-ice extent trend. A related climate extreme was the return of the Weddell Polynya in 2016 and 2017[230]. Later, in February 2022, the sea ice extent dropped to lowest ever observed during the satellite-era since 1978. Negative sea ice anomalies occurred in all sectors of the Southern Ocean[231].

Perhaps the most dramatic Antarctic climate extremes have been the collapses of the Larsen A, Larsen B, and Wilkins ice shelves in the Antarctic Peninsula[232–234]. Collapses of ice shelves have often accelerated the downslope flow of the upstream glaciers[235], contributing to the global sea level rise.

Table 1

	+/-1.5 Standard Deviation (Pre~2000)	Probability (%)		+/-1.5 Standard Deviation (1984/85-2013/14)	Probability (%)		
		Pre-2000	Post-2000		1984/85-2013/14	2014/15-2044/45	2069/70-2098/99
SAT (°C)	-11.47	8.2	28.2	-10.58	6.7	23.5	79.3
Precipitation (mm d^{-1})	2.13	7.4	11.1	1.44	6.7	17.3	55.8
Ocean Heat Transport (TW)	332.1	6.7	16.1	-	-	-	-
Atlantic Layer Temperature (°C)	0.88	6.7	83.3	2.10	6.7	18.3	75.4
Mixed Layer Temperature (°C)	0.12	6.7	81.5	1.43	6.7	28.5	83.2
SST Anomaly (°C)	1.62	6.7	66.8	-	-	-	-
Sea Ice Loss (x10^6 km^2)	-2.18	6.7	90.2	-3.89	6.7	50.7	-
GrIS melt extent (x10^6 km^2)	3.29	6.7	69.6	-	-	-	-
GrIS melt rate (m yr^{-1})	-	-	-	0.66	6.7	57.2	100%

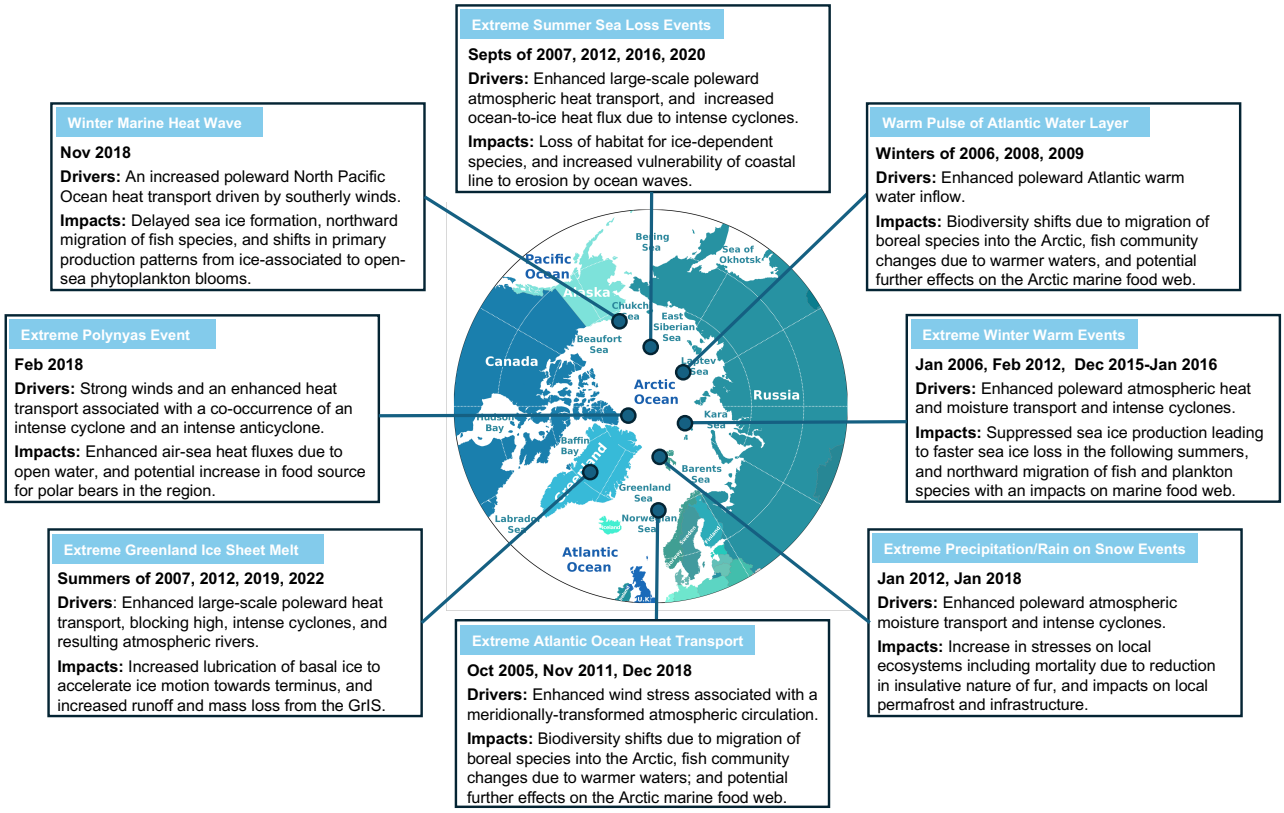

Figure 1. **Summary of selected striking Arctic rare weather and climate extremes and impacts.** Striking rare weather and climate extreme events have consistently and systematically occurred across the Arctic climate system from the atmosphere to the ocean and cryosphere since the beginning of the 21st century. Their occurrence spans the whole Arctic region from the North Atlantic Arctic to the North Pacific Arctic and Greenland. Impacts are not only limited within one climate system component in which extreme events occur, but also on other components and Arctic ecosystem, permafrost, and infrastructures, which have significant implications for economy and society. [Striking and highly impactful rare weather and climate extremes have been observed in the Arctic climate system].

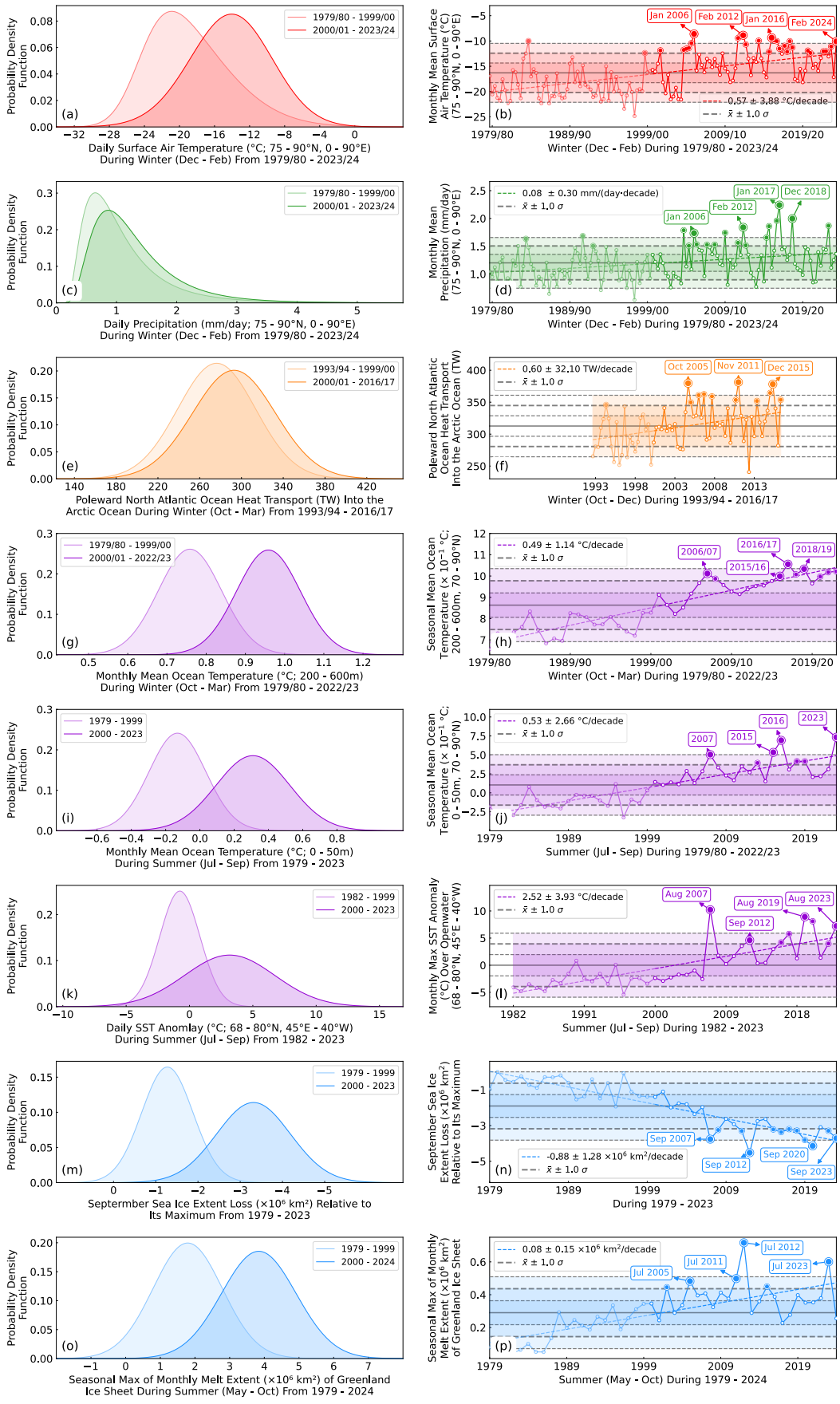
(a)
1979/80 - 1999/00
2000/01 - 2023/24
Probability Density Function
Daily Surface Air Temperature (°C; 75 - 90°N, 0 - 90°E) During Winter (Dec - Feb) From 1979/80 - 2023/24
(b)
Jan 2006
Feb 2012
Jan 2016
Feb 2024
0.57 ± 3.88 °C/decade
x̄ ± 1.0 σ
Monthly Mean Surface Air Temperature (°C) (75 - 90°N, 0 - 90°E)
Winter (Dec - Feb) During 1979/80 - 2023/24
(c)
1979/80 - 1999/00
2000/01 - 2023/24
Daily Precipitation (mm/day; 75 - 90°N, 0 - 90°E) During Winter (Dec - Feb) From 1979/80 - 2023/24
(d)
0.08 ± 0.30 mm/(day·decade)
Jan 2017
Dec 2018
Feb 2012
Jan 2006
Monthly Mean Precipitation (mm/day) (75 - 90°N, 0 - 90°E)
(e)
1993/94 - 1999/00
2000/01 - 2016/17
Poleward North Atlantic Ocean Heat Transport (TW) Into the Arctic Ocean During Winter (Oct - Mar) From 1993/94 - 2016/17
(f)
0.60 ± 32.10 TW/decade
Oct 2005
Nov 2011
Dec 2015
Poleward North Atlantic Ocean Heat Transport Into the Arctic Ocean (TW)
Winter (Oct - Dec) During 1993/94 - 2016/17
(g)
1979/80 - 1999/00
2000/01 - 2022/23
Monthly Mean Ocean Temperature (°C; 200 - 600m) During Winter (Oct - Mar) From 1979/80 - 2022/23
(h)
0.49 ± 1.14 °C/decade
2006/07
2016/17
2018/19
2015/16
Seasonal Mean Ocean Temperature (× 10⁻¹ °C; 200 - 600m, 70 - 90°N)
Winter (Oct - Mar) During 1979/80 - 2022/23
(i)
1979 - 1999
2000 - 2023
Monthly Mean Ocean Temperature (°C; 0 - 50m) During Summer (Jul - Sep) From 1979 - 2023
(j)
0.53 ± 2.66 °C/decade
2007
2015
2016
2023
Seasonal Mean Ocean Temperature (× 10⁻¹ °C; 0 - 50m, 70 - 90°N)
Summer (Jul - Sep) During 1979/80 - 2022/23
(k)
1982 - 1999
2000 - 2023
Daily SST Anomlay (°C; 68 - 80°N, 45°E - 40°W) During Summer (Jul - Sep) From 1982 - 2023
(l)
2.52 ± 3.93 °C/decade
Aug 2007
Aug 2019
Aug 2023
Sep 2012
Monthly Max SST Anomaly (°C) Over Openwater (68 - 80°N, 45°E - 40°W)
Summer (Jul - Sep) During 1982 - 2023
(m)
1979 - 1999
2000 - 2023
Septermber Sea Ice Extent Loss (×10⁶ km²) Relative to Its Maximum From 1979 - 2023
(n)
-0.88 ± 1.28 ×10⁶ km²/decade
Sep 2007
Sep 2012
Sep 2020
Sep 2023
September Sea Ice Extent Loss (×10⁶ km²) Relative to Its Maximum
During 1979 - 2023
(o)
1979 - 1999
2000 - 2024
Seasonal Max of Monthly Melt Extent (×10⁶ km²) of Greenland Ice Sheet During Summer (May - Oct) From 1979 - 2024
(p)
0.08 ± 0.15 ×10⁶ km²/decade
Jul 2005
Jul 2011
Jul 2012
Jul 2023
Seasonal Max of Monthly Melt Extent (×10⁶ km²) of Greenland Ice Sheet
Summer (May - Oct) During 1979 - 2024

Figure 2. **Observed changes in rare extreme events across the Arctic climate system components**. **a** | The probability density function (PDF) distributions of winter (December - February) daily surface air temperature (SAT) over the North Atlantic Arctic (75°N - 90°N, 0 - 90°E) for the time periods of 1979/80 - 1999/2000 and 2000/01 - 2023/24. **b** | The time series of the winter (December - February) monthly mean SAT from 1979/80 - 2023/24. **c** | The same as **a**, but for precipitation. **d** | The same as **b**, but for precipitation. The North Atlantic Arctic is chosen in panels **a** - **d** because rare extreme warm and heavy precipitation events have more frequently occurred in this area from the observations. Datasets employed in the analysis shown by **a** - **d** are from the fifth generation of the European Centre for Medium-Range Weather Forecasts (ECMWF) atmospheric reanalysis (ERA5)[243]. **e** | The PDF distributions of winter (October - March) poleward North Atlantic oceanic heat transport into the Arctic Ocean and Nordic Seas for the time periods of 1993/94 - 1999/2000 and 2000/01 - 2016/17. **f** | The time series of winter poleward North Atlantic oceanic heat transport into the Arctic Ocean and Nordic Seas from 1993/94 - 2016/17. The data used in **e** and **f** are from ref 53. **g** | The PDF distributions of winter (October - March) Atlantic water layer temperature (thickness-weighted vertical average between 200 - 600 m) within the central Arctic (north of 70°N) for the time periods of 1979/80 - 1999/2000 and 2000/21 - 2022/23. **h** | The time series of winter Atlantic water layer temperature form 1979/80 - 2022/23. **i** | The same as **g**, but for summer (July - September) upper ocean mixed layer temperature (thickness-weighted vertical average between 0 - 50 m) for the time periods of 1979 - 1999 and 2000 - 2023. **j** | The same as **h**, but for the summer upper ocean mixed layer temperature from 1979 - 2023. Three-dimensional ocean temperature data are from ref 57. **k** | The PDF distributions of summer (July - September) area-weighted sea surface temperature (SST) in the summer open water and marginal ice zone area (70°N - 90°N) for the time periods of 1982 - 1999 and 2000 - 2023. **l** | The time series of summer area-weighted SST in the summer open water and marginal ice zone area from 1982 - 2023. The SST data in **k** and **l** are from https://www.ncei.noaa.gov/products/optimum-interpolation-sst[244]. **m** | The PDF distributions of September sea ice extent relative to its maximum for the time periods of 1979 - 1999 and 2000 - 2023. **n** | The time series of September sea ice extent relative to its maximum from 1979 - 2023. The sea ice extent relative to its maximum is chosen to clearly delineate sea ice extent loss. The maximum value is identified from the data during 1979 - 1999. The sea ice extent in **m** and **n** is derived from the sea ice concentration (> 15%) dataset[78]. **o** | The PDF distributions of the summer (May - October) seasonal maximum of monthly Greenland Icesheet melt extent for the time periods of 1979 - 1999 and 2000 - 2023. **p** | The time series of the summer seasonal maximum of monthly Greenland Icesheet melt extent form 1979 - 2023. Data analyzed in **o** and **p** are from the National Snow & Ice Data Center (https://nsidc.org/greenland-today/greenland-surface-melt-extent-interactive-chart/; reproduced from ref [245]). In the time series panels, the straight dashed lines indicate linear trends. The three layers of shading represent the ranges of climate fluctuation from ± 1.0 to ± 1.5 σ throughout the analysis periods. The threshold of ± 1.0 σ is highlighted by horizontal dashed lines. A number of months or years are marked showing the times when selected striking rare extreme events occur in each panel of time series. Light colors and deep colors are used in the lines of time series to highlight the periods before and after the turn of the 21st century, respectively. A coherent increase in the frequency and intensity of extreme events since the beginning of the 21st century can be clearly seen across the time series panels. [An increase in the frequency of Arctic weather and climate extremes that exceed at least +1.0 σ of their historical variability have coherently occurred across the Arctic climate system components since the turn of the 21st century].

(a) Present-day

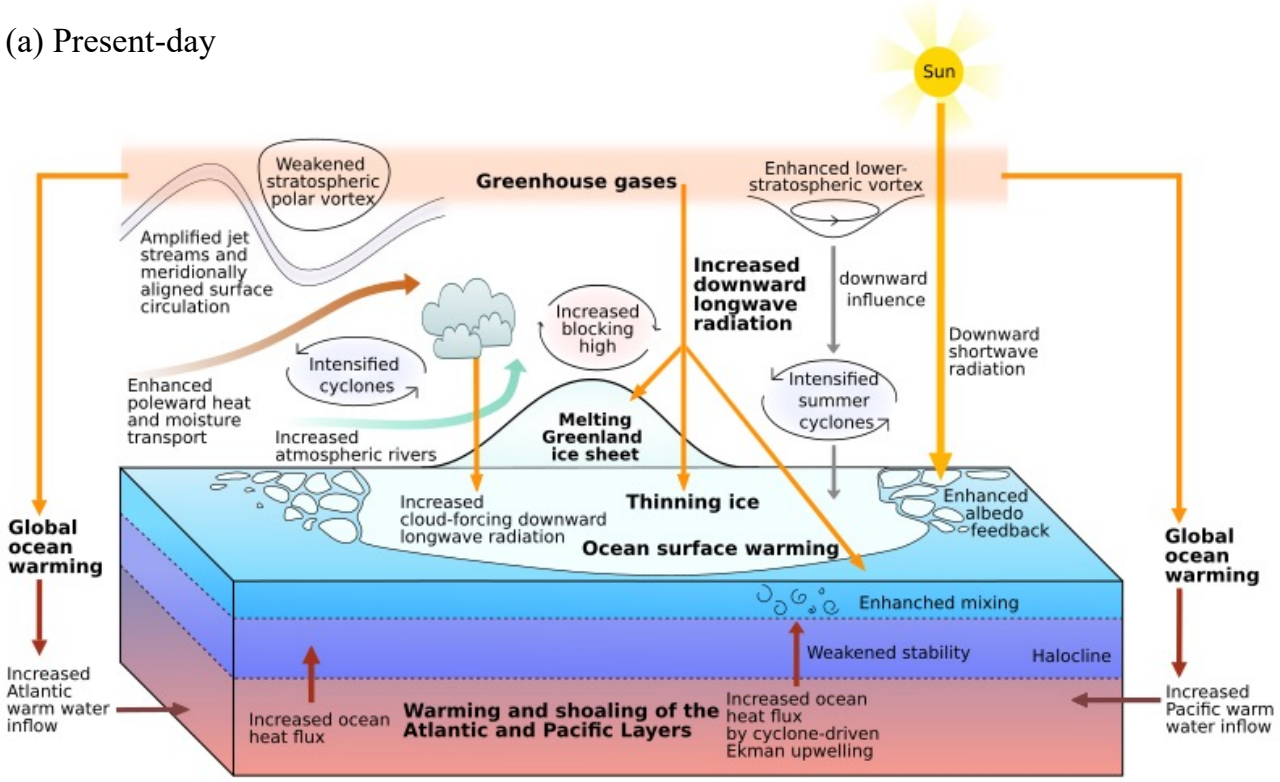

(b) Projected Future

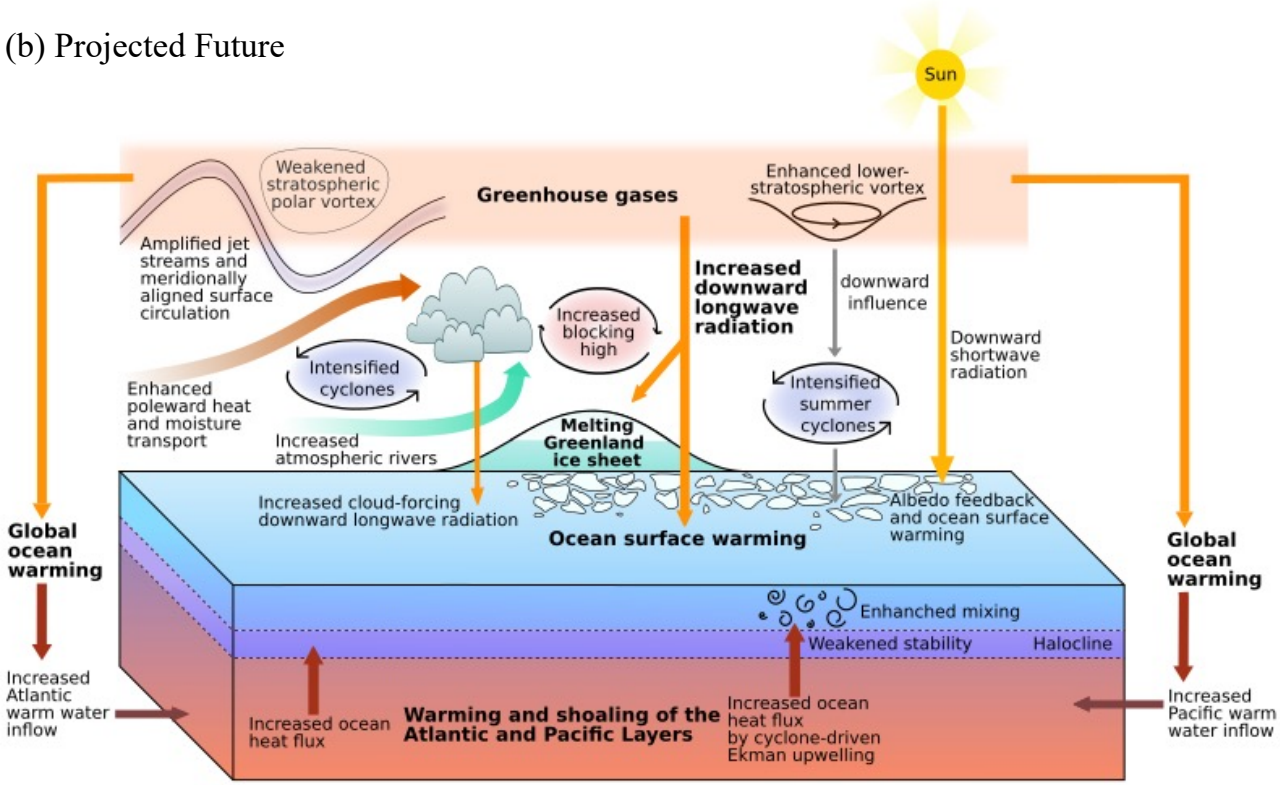

Figure 3. **Schematics showing multiscale "pushing and triggering" mechanisms driving the occurrence of extremes across the Arctic climate system. a** | For present-day: The increased greenhouse gas emissions forcing plays a "pushing" role in elevating the baselines of the Arctic climate system, characterized by an increase in atmosphere, ocean, sea ice, and Greenland ice sheet temperatures, which correspondingly result in

a shrunken sea ice extent, thinned sea ice thickness, and reduced Greenland ice sheet mass (denoted by bold fonts). Meanwhile, key large-scale and synoptic-/meso-scale atmospheric, ocean, and sea ice dynamic and thermodynamic processes play a "triggering" role in driving the occurrence of Arctic extremes. These processes not only take effect within each component of the Arctic climate system and across the Arctic atmosphere-ocean-sea ice interfaces, but also link the Arctic to the lower-latitudes. Specially, the stratospheric polar vortex weakens and shifts southward, the jet stream waves are amplified, and the large-scale atmospheric circulation is meridionally transformed, enhancing poleward heat and moisture transport into the Arctic; cyclone and blocking high activity intensifies, increasing the occurrence of atmospheric rivers; cloud-forced downward longwave radiation increases due to an enhanced poleward moisture transport and increased atmospheric rivers; poleward North Atlantic and North Pacific warm water inflows intensify by the meridionally-aligned atmospheric circulation; ocean mixing in the upper ocean mixed layer and Ekman upwelling of deeper layer warm water increase due to intensified cyclone activity; and sea ice-albedo feedback is enhanced as a consequence of declining sea ice. A more complete, interpretative diagram can be found in Supplementary Fig. S10, delineating how the multiscale atmosphere, ocean, sea ice processes and their interactive and feedback processes work together to synergistically drive the occurrence of Arctic extremes. **b** | The same as **a**, but for the projected future: The projected greenhouse gas emissions forcing is increased to a higher level than present-day, which "pushes" the Arctic climate system to a further warmed state and strengthens the "triggering" roles of the changed atmosphere, ocean, and sea ice processes and feedbacks in the occurrence of Arctic extremes. [Global warming and nonlinear atmosphere, ocean, and sea ice dynamics play "pushing and triggering" roles in driving the increased frequency of occurrence of Arctic weather and climate extremes].

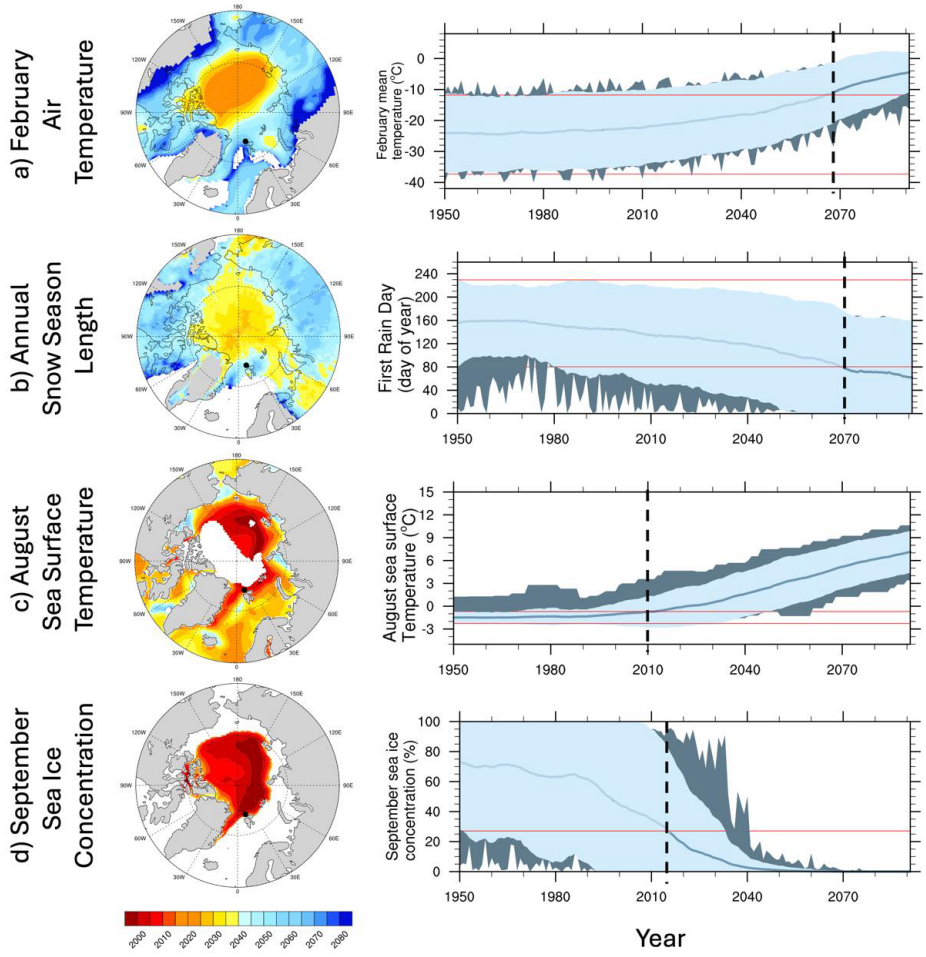

Figure 4. **Projected Time of Emergence in the Arctic**. **a** | Time of Emergence (ToE) for February SAT over the Arctic (left) and at a selected point north of Svalbard (right; black dot on the left map). **b** | The same as **a**, but for the length of annual snow season (left) and the first day of annual rain season (right). **c** | The same as **a**, but for August sea surface temperature (SST). **d** | The same as **a**, but for September sea ice concentration. The ToE is defined as the year when the model ensemble mean (blue solid line) crosses the ±2.0 standard deviation (red solid lines) from the baseline climate state. The baseline climate state is the mean climate state during 1920 - 1929. The year of ToE for all variables is shown by the dashed back line in the time series panels on the right. All data are from the Community Earth System Model version 1 Large Ensemble (CESM-LE)[202]. The projected ToE represents an extreme change of a projected climate state surpassing the ±2.0 standard deviation range of the baseline climate variability. [An extreme shift can occur in the state of the Arctic climate system largely beyond what the baseline climate variability explains].

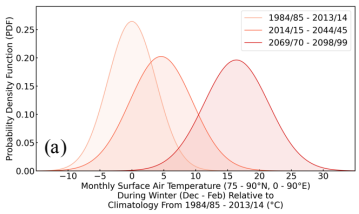
1984/85 - 2013/14
2014/15 - 2044/45
2069/70 - 2098/99
Probability Density Function (PDF)
(a)
Monthly Surface Air Temperature (75 - 90°N, 0 - 90°E)
During Winter (Dec - Feb) Relative to
Climatology From 1984/85 - 2013/14 (°C)

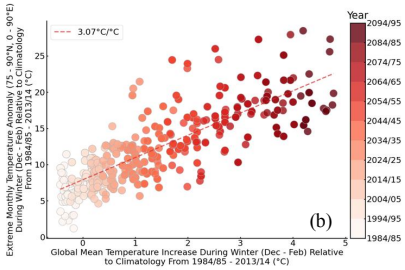
3.07°C/°C
Year
(b)
Extreme Monthly Temperature Anomaly (75 - 90°N, 0 - 90°E)
During Winter (Dec - Feb) Relative to Climatology
From 1984/85 - 2013/14 (°C)
Global Mean Temperature Increase During Winter (Dec - Feb) Relative
to Climatology From 1984/85 - 2013/14 (°C)

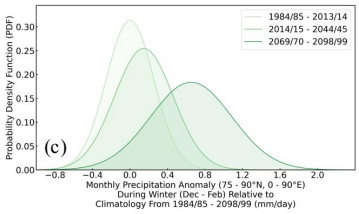
1984/85 - 2013/14
2014/15 - 2044/45
2069/70 - 2098/99
Probability Density Function (PDF)
(c)
Monthly Precipitation Anomaly (75 - 90°N, 0 - 90°E)
During Winter (Dec - Feb) Relative to
Climatology From 1984/85 - 2098/99 (mm/day)

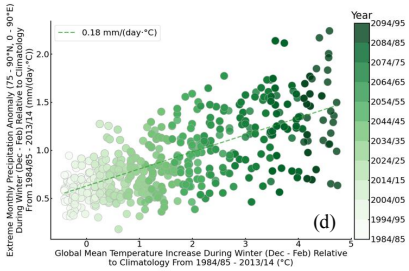
0.18 mm/(day·°C)
Year
(d)
Extreme Monthly Precipitation Anomaly (75 - 90°N, 0 - 90°E)
During Winter (Dec - Feb) Relative to Climatology
From 1984/85 - 2013/14 (mm/(day·°C))
Global Mean Temperature Increase During Winter (Dec - Feb) Relative
to Climatology From 1984/85 - 2013/14 (°C)

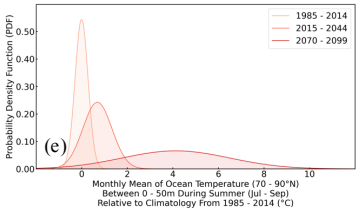
1985 - 2014
2015 - 2044
2070 - 2099
Probability Density Function (PDF)
(e)
Monthly Mean of Ocean Temperature (70 - 90°N)
Between 0 - 50m During Summer (Jul - Sep)
Relative to Climatology From 1985 - 2014 (°C)

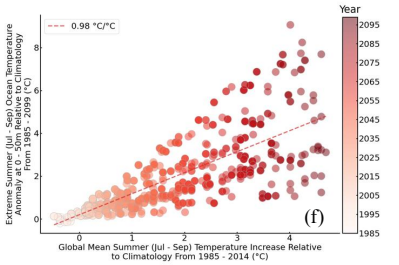
0.98 °C/°C
Year
(f)
Extreme Summer (Jul - Sep) Ocean Temperature
Anomaly at 0 - 50m Relative to Climatology
From 1985 - 2099 (°C)
Global Mean Summer (Jul - Sep) Temperature Increase Relative
to Climatology From 1985 - 2014 (°C)

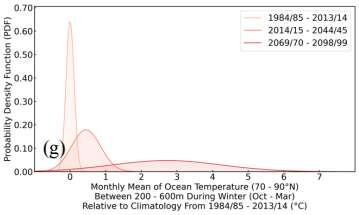
1984/85 - 2013/14
2014/15 - 2044/45
2069/70 - 2098/99
Probability Density Function (PDF)
(g)
Monthly Mean of Ocean Temperature (70 - 90°N)
Between 200 - 600m During Winter (Oct - Mar)
Relative to Climatology From 1984/85 - 2013/14 (°C)

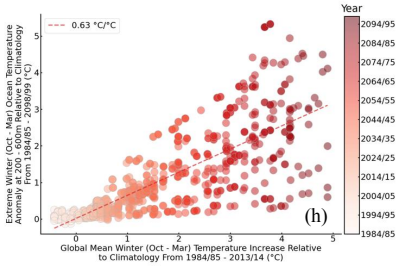
0.63 °C/°C
Year
(h)
Extreme Winter (Oct - Mar) Ocean Temperature
Anomaly at 200 - 600m Relative to Climatology
From 1984/85 - 2098/99 (°C)
Global Mean Winter (Oct - Mar) Temperature Increase Relative
to Climatology From 1984/85 - 2013/14 (°C)

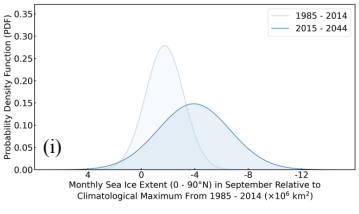
1985 - 2014
2015 - 2044
Probability Density Function (PDF)
(i)
Monthly Sea Ice Extent (0 - 90°N) in September Relative to
Climatological Maximum From 1985 - 2014 (×10⁶ km²)

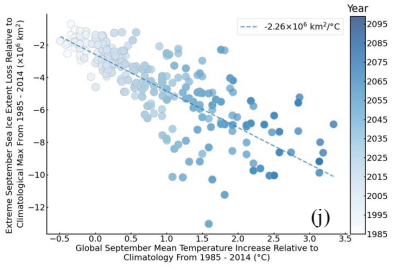
-2.26×10⁶ km²/°C
Year
(j)
Extreme September Sea Ice Extent Loss Relative to
Climatological Max From 1985 - 2014 (×10⁶ km²)
Global September Mean Temperature Increase Relative to
Climatology From 1985 - 2014 (°C)

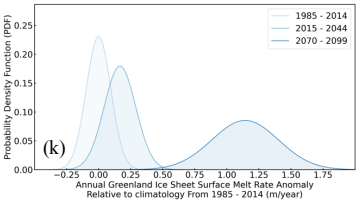
1985 - 2014
2015 - 2044
2070 - 2099
Probability Density Function (PDF)
(k)
Annual Greenland Ice Sheet Surface Melt Rate Anomaly
Relative to climatology From 1985 - 2014 (m/year)

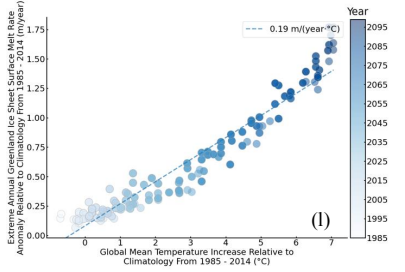
0.19 m/(year·°C)
Year
(l)
Extreme Annual Greenland Ice Sheet Surface Melt Rate
Anomaly Relative to Climatology From 1985 - 2014 (m/year)
Global Mean Temperature Increase Relative to
Climatology From 1985 - 2014 (°C)

Figure 5. **Projected future changes in Arctic extremes. a** | The probability density function (PDF) distributions of winter (December - February) daily surface air temperature (SAT) anomaly over the North Atlantic Arctic (75°N - 90°N; 0 - 90°E) for the three 30-year time periods of 1984/85 - 2013/14, 2014/15 - 2044/45, and 2069/70 - 2098/99. **b** | Changes of extreme warm events (SAT anomaly exceeding a threshold of +2.0 standard deviation) with the global mean SAT increase. **c** | The same as **a**, but for precipitation. **d** | The same as **b**, but for precipitation. **e** | The PDF distributions of summer (July - September) monthly upper ocean mixed layer temperature (thickness-weighted between 0 - 50 m) anomaly in the central Arctic (70°N – 90°N) for the three 30-year time periods of 1985 - 2014, 2015 - 2045, and 2070 - 2099. **f** | Changes of summer upper ocean mixed layer extreme warm events (ocean temperature anomaly exceeding a threshold of +1.5 standard deviation) with the global mean SAT increase. **g** | The same as **e**, but for winter (October – March) Atlantic water layer ocean temperature (thickness-weighted between 200 – 600 m) for the three 30-year time periods of 1984/85 - 2013/14, 2014/15 - 2044/45, and 2069/70 - 2098/99. **h** | The same as **f**, but for winter North Atlantic water layer extreme warm events. **i** | The PDF distributions of September monthly sea ice extent relative to the maximum during 1985-2014 for the two 30-year time periods of 1985 – 2014 and 2015 - 2045. Considering the projected ice-free Arctic Ocean after the mid 21st century, the PDF analysis does not cover the time period from 2070 - 2099. **j** | Changes of extreme September sea ice extent loss events (sea ice extent anomaly exceeding a threshold of +1.5 standard deviation) with the global mean SAT increase. **k** | The PDF distributions of annual Greenland Ice Sheet surface melt rate anomaly for the three 30-year time periods of 1985 – 2014, 2015 – 2045, and 2070 - 2099. **l** | Changes of extreme Greenland Ice Sheet surface melt rate events (surface melt rate anomaly exceeding a threshold of +1.5 standard deviation) with the global mean SAT increase. All data used in panels a - j are from the CMIP6 multi-model projections[208]. The employed models are listed in Supplementary Table S2. To reduce interconnections between model projections, only one ensemble member was chosen from each model. The data in panels **k** and **l** are from ref [209]. The extreme events are identified using a moving 20-year time window with an interval of 5-year between two windows. The statistical distributions show a continuing, coherent shift of the Arctic climate system to a further warmed states, increasing the likelihood of the occurrence of extremes. The scatter plots suggest intensification of extreme events across the Arctic climate system. [Arctic weather and climate extremes are projected to more frequently occur and to be exacerbated in the future].

Box 1 | **Antarctic weather and climate extremes**

In the circumpolar scale, recent evolution of the Antarctic climate system has been characterized as having less dramatic changes than those occurring in the Arctic. However, regional weather and climate extremes have been prominent in the Antarctic[246].

The record-lowest 2-m air temperature observed in the Antarctic dates back to 21 July 1983, when -89.2°C was observed at the Vostok station in East Antarctica. Due to the sparsity of observations, it does not necessarily represent the coldest weather event in Antarctica. Satellite thermal infrared mapping has revealed snow surface temperatures of approximately -98°C in several small topographic basins in high-elevation East Antarctica during winters of 2004–2016[247]. These were estimated to correspond to 2-m air temperatures of approximately -94°C. The warmest 2-m air temperature ever observed in the Antarctic continent, 18.3°C, occurred at the Argentinian Esperanza station on the northern tip of the Antarctic Peninsula on 6 February 2020. The event was associated with anticyclonic circulation bringing a warm, moist air mass from the Pacific Ocean to the Antarctic Peninsula, and a strong Foehn downslope of the Peninsula mountains made the downslope flow record warm[248]. An extreme heatwave occurred over East Antarctica on 15-19 March 2022. Widespread warm anomalies reached 30-45°C, driven by an extremely intense atmospheric river[249,250]. It transported heat and moisture from the sea south of Australia far to the high plateau of East Antarctica. In addition to extreme temperatures, atmospheric rivers are often responsible for extreme precipitation events in coastal regions of Antarctica[251]. Such events have become more common and more intense[252].

A prominent climate extreme was the sudden decline of Antarctic sea-ice extent in late 2016, after three decades of increase. The decline was preconditioned by warming of surface waters and thinning of sea ice in the Southern Ocean, and occurred due to extreme atmosphere-ocean anomalies in the eastern tropical Indian

and far-western Pacific Oceans[253]. These anomalies triggered atmospheric planetary wave trains that propagated to the Antarctic, generated wind anomalies, changed the sea-ice patterns, and reversed the hemispheric sea-ice extent trend. A related climate extreme was the return of the Weddell Polynya in 2016 and 2017[254]. Later, in February 2022, the sea ice extent dropped to lowest ever observed during the satellite-era since 1978. Negative sea ice anomalies occurred in all sectors of the Southern Ocean[255].

Perhaps the most dramatic Antarctic climate extremes have been the collapses of the Larsen A, Larsen B, and Wilkins ice shelves in the Antarctic Peninsula[256–258]. Collapses of ice shelves have often accelerated the downslope flow of the upstream glaciers[259], contributing to the global sea level rise.